Validation of FLACS for Vapor Dispersion from LNG Spills: Model Evaluation Protocol

Olav R. Hansen, Mathieu Ichard and Scott G. Davis*
GexCon US, 7735 Old Georgetown Rd suite 1010, Bethesda, MD 20814
***Email: sgdavis@gexcon.com**

Abstract

Since LNG spills are complex phenomena and may occur on scales much larger than are assessable to experiment, models have been utilized to help evaluate hazards associated with LNG releases. This has led to the development of a Model Evaluation Protocol (MEP) that can be used to assess the suitability of dispersion models for predicting hazard ranges associated with large spills of LNG. The hazards associated with LNG releases are usually analyzed in three phases: the source term or the development of the evaporating LNG pool, atmospheric dispersion or the transport of the natural gas vapors, and effects (whether thermal radiation or explosion consequences). Traditionally the source term is analyzed separately from the dispersion model, where the output from the source model is used as input in the dispersion model. However, recent research has demonstrated that some widely accepted source and dispersion models are physically inaccurate, as they do not allow for realistic pool spreading, do not allow for air entrainment or heating of the evaporating gas, and do not properly account for obstacles. Furthermore, the source and dispersion processes are integrated processes that occur during an LNG release. An alternate approach is to apply computation fluid dynamics (CFD) to both the spill and dispersion model, as they can take into account the combined physical phenomena associated with LNG releases. FLACS is one of the few CFD models with integrated source and dispersion models. This paper presents the validation work of FLACS, widely used for consequence modeling in the oil and gas industry, against all of the benchmarks outlined in the MEP. FLACS was used to simulate the obstructed and unobstructed cases, including both the wind tunnel experiments and large-scale field trials. FLACS predictions were compared with specific datasets and FLACS successfully met the quantitative assessment criteria for the validation stage of the MEP.

Background

Due to the scales and complexity oftentimes associated with liquefied natural gas (LNG) spills, models have been utilized to help evaluate hazards associated with LNG releases. This has led to the development of a Model Evaluation Protocol (MEP), (Ivings *et al*., 2007) which can be used to assess the suitability of dispersion models for predicting hazard ranges associated with large spills of LNG. The hazards and consequences associated with LNG releases are typically evaluated in three phases: the source term or the spill and development of the evaporating LNG pool, atmospheric dispersion or the transport of the natural gas vapors, and the effects that could include thermal radiation or explosion consequences. The source term, which occurs immediately after and during the release, is dominated by: conditions under which the LNG is stored or transported, the type of failure and release conditions, and the surrounding terrain upon

which the LNG is released (water, concrete, or other surface). The transport of the natural gas vapors is dominated by factors such as the local terrain and atmospheric conditions.

Traditionally in LNG hazard assessments the source term is modeled separately from the dispersion model, whereas the output from the source model or the vapor generation of the fluid at that state is used as input into the dispersion model. However, recent research has shown that some of the more implemented source term and dispersion models are physically inaccurate regarding pool spreading phenomena, do not allow for realistic pool spreading, do not allow for air entrainment or heating of the evaporating gas, and do not properly account for obstacles (Webber *et al*., 2009). LNG dispersion models need to include the physical phenomena associated with cold, denser-than-air vapor clouds, including complex terrain (mountains, valleys, etc.). Furthermore, the source and dispersion models are integrated processes that occur during an LNG release and it has been recognized that the source model can have a significant impact on the dispersion results (see Koopman *et al*., 2007; Webber *et al*., 2009).

Recognizing the importance of LNG hazard assessment, the Fire Protection Research Foundation (FPRF) undertook a research project to develop tools for the National Fire Protection Agency (NFPA) Liquefied Natural Gas Technical Committee to evaluate LNG dispersion models. This work was carried out by the Health and Safety Laboratory (HSL) and they delivered a Model Evaluation Protocol (MEP), which contained a structure for complete model evaluation (Ivings *et al*., 2007). The idea being that all models would need to be validated against key experimental data and is a key part of the model evaluation. The Model Validation Database (Coldrick *et al*., 2009) provides the means to undertake a structured and rigorous quantitative evaluation of the performance of LNG dispersion models by comparisons with measurements. The Model Validation Database consists of both large-scale field trials as well as wind tunnel tests.

The field trials are primarily releases of LNG (Maplin Sands, Burro, Coyote and Falcon), supplemented by two tests from the Thorney Island releases of Freon (McQuaid, 1987). The latter set of trials includes releases in stable atmospheric conditions, whereas the LNG field trials data is largely restricted to neutral or unstable conditions with the exception of the Burro test 8 which was performed under stable atmospheric conditions. All of these field trials releases are over unobstructed terrain, with the exception of the Falcon trials in which a large fence surrounded the LNG source. To ensure that the Model Validation Database is appropriate for the evaluation of LNG dispersion models which account for the effect of obstructions, it also contains data from wind tunnel tests of dense gas releases in the presence of obstacles. These wind tunnel tests comprise recent work undertaken at the Chemical Hazards Research Center at the University of Arkansas (Havens & Spicer, 2005, 2006, 2007), as well as two series of tests carried out as part of European Commission-funded projects, referred to as BA-Hamburg and BA-TNO (Nielsen & Ott, 1996; Schatzmann *et al*., 1991).

An alternate approach to LNG hazard assessment would be to apply computation fluid dynamics (CFD) to both the spill and dispersion model (see Luketa-Hanlin *et al*., 2007), consistent with recent findings (Webber *et al.*, 2009). FLACS is one of the few CFD models with integrated source and dispersion models. The source model is a 2D shallow water model and couple with a 3D dispersion model that has been extensively validated against experiments. FLACS is widely used for consequence modeling in the oil and gas industry. This paper will first present a

description of both the source and dispersion models used in FLACS. Next, the validation work of FLACS will be presented against all of the benchmarks outlined in the MEP, which include both the large-scale field trials and the wind tunnel experiments. The results for the unobstructed tests will be presented first followed by the obstructed tests. Based on the validation results, FLACS has successfully met the quantitative assessment criteria for the validation stage of the MEP. Comments are also provided in areas where improvement between predictions and experiment may be attained.

FLACS CFD Model

Source – Pool Spread and Evaporation Model

FLACS incorporates a pool model that allows for the formation and spreading of the pool, with local evaporation rates based on the heat transfer from the ground or water, radiation, local wind speeds and turbulence levels, and the local vapor pressure above the pool (Hansen *et al*., 2007). Figure 1 shows a schematic of the physical processes modeled in the FLACS source model.

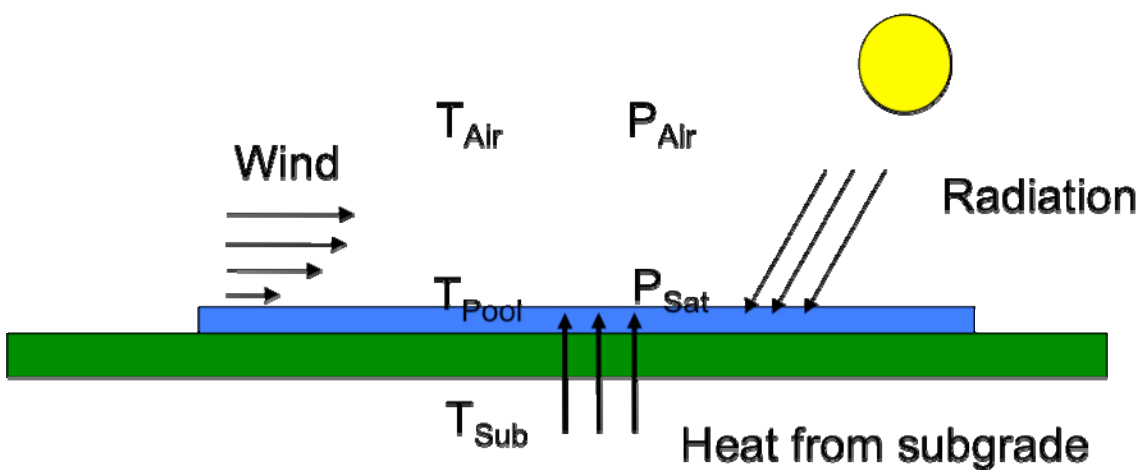

Figure 1: Schematic of the physical processes modeled in FLACS

The 2D Shallow Water Equations are implemented in the LNG source model. These equations take into account the influence of surrounding obstacles on the spread of the pool. The equation solved for the spill height is given by:

$$\frac{\partial h}{\partial t} + \frac{\partial h u_i}{\partial x_i} = \frac{\dot{m}_L - \dot{m}_V}{\rho_l} \tag{1}$$

and the momentum equation is written as:

$$\frac{\partial u_i}{\partial t} + u_j \frac{\partial u_i}{\partial x_j} = F_{g,i} + F_{\tau,i}\,, \tag{2}$$

$$F_{g,i} = g\Delta \frac{\partial(h+z)}{\partial x_i}, \tag{3}$$

where the elevation of the ground has also been included. The parameter Δ equals one for solid surfaces and $\Delta = (1-\rho_l/\rho_w)$ for spills on water. The shear stress between the spill and substrate is given by the general formula:

$$F_{\tau,i} = \frac{1}{8} f_f u_i |\vec{u}| \tag{4}$$

The transport equation for the specific enthalpy is given by:

$$\frac{\partial \theta}{\partial t} + u_i \frac{\partial \theta}{\partial x_i} = \frac{\dot{m}_L}{h}(\theta_L - \theta) + \dot{q}_c + \dot{q}_{rad} + \dot{q}_g + \dot{q}_{evap} \tag{5}$$

The first term on the right hand side is due to the leak, $\dot{q}_c$ is convective heat transfer, $\dot{q}_{rad}$ is heat transfer to the pool from radiation, $\dot{q}_g$ is heat transfer to the pool from the substrate, and $\dot{q}_{evap}$ is heat loss due to evaporation. Heat transfer from the solid and rough ground (soil and concrete) is approximated by:

$$\dot{q}_{q,solid} = \begin{cases} \dfrac{\lambda_G (T_G^0 - T_l)(1.5 - 0.25(t - t_{GW})}{\sqrt{\pi \alpha_G}} & \text{if } t < 4 \text{ sec.} \\ \dfrac{\lambda_G (T_G^0 - T_l)}{\sqrt{\pi \alpha_G (t - t_{GW})}} & \text{if } t \geq 4 \text{ sec.} \end{cases} \tag{6}$$

In Equation (6), λ_G is the thermal conductivity of the ground, α_G is the thermal diffusivity of the ground and t_{GW} is the time at which the ground is wetted. Infinite ground depth is assumed in the derivation of the expressions for the heat transferred from the ground in Equation (6).

Boiling LNG on water can take place in transition boiling and film boiling regimes. Conrado & Vesovic (2000) proposed correlations for film and transition boiling for non-moving liquids. Experiments have shown that the heat transfer coefficient is considerable higher for LNG on the sea than estimated by the correlations for non-moving pools. Heat transfer enhancement for spills on water is primarily due to the turbulent mixing between LNG and water as the LNG impinges the water surface. Hissong (2007) introduced a turbulence factor to model the film instability and the increased contact area between LNG and water. In the present work, the local Reynolds number is used to calculate the effective heat transfer rate:

$$\dot{q}_{g,water} = \begin{cases} \dot{q}_{\text{film}} & \text{, if} \quad \text{Re}_h < 15 \\ \frac{1}{2}\dot{q}_{\text{film}} + \frac{1}{2}\left(\dot{q}_{\text{film}}\left(\frac{1500-\text{Re}_h}{1485}\right) + \dot{q}_{cb}\left(\frac{\text{Re}_h - 15}{1486}\right)\right) & \text{, if} \quad 15 < \text{Re}_h < 1500 \\ \frac{1}{2}\dot{q}_{\text{film}} + \frac{1}{2}\dot{q}_{cb} & \text{, if} \quad \text{Re}_h > 1500 \end{cases} \tag{7}$$

where $\dot{q}_{\text{film}}$ refers to the heat transfer for non-moving liquids calculated by the correlations in Conrado & Vesovic (2000) and $\dot{q}_{cb}$ is the convective heat transfer that is calculated as follows:

$$\dot{q}_{cb} = 0.0133\,\text{Re}_h^{0.69}\,\text{Pr}_l^{0.4}\,\frac{\lambda_l}{h}(T_W - T_l) \tag{8}$$

The governing equations for the spill are discretized on a non-uniform Cartesian staggered grid in two dimensions with a finite volume method. A first-order upwind scheme is employed for the convective terms in the momentum equation, while a central difference scheme is used for the enthalpy equation. The equations are solved explicitly in time with a 3rd order Runge-Kutta solver.

Dispersion Model

The dispersion models in FLACS have been extensively validated against dispersion and explosion experiments. FLACS is predominately used in the oil and gas industry to help evaluate the hazards associated with offshore and onshore facilities. FLACS has been developed in collaboration with many industries and is used by over 60 organizations worldwide. FLACS has been tested for a wide range of different dispersion scenarios including releases of dense, passive and buoyant gases in open, obstructed and enclosed spaces (see Hanna *et al*., 2004; Dharmavaram *et al*., 2005; Flaherty *et al*., 2007; Hanna *et al*., 2009). FLACS features a distributed porosity model for small, sub-grid scale obstacles, a semi-automated process for creating complex flow geometry (CAD import) and a simple Cartesian grid that enables simulations to be produced more rapidly than for many other general-purpose CFD codes.

FLACS solves the Reynolds Averaged Navier-Stokes equations by using the *k*-*ε* model with the standard set of constants taken from Launder & Spalding (1974) for the turbulent closure. Buoyancy effects are taken into account in the turbulent equations. The atmospheric boundary

layer is modeled by forcing profiles for the velocity, temperature and the turbulence parameters on inlet boundaries. Wind inlet profiles rely on the Monin-Obukhov length L and the atmospheric roughness length z_0. The Monin-Obukhov length can be estimated from measurements and it is positive for stable atmospheric boundary layers, negative for unstable boundary layers and infinity for neutral boundary layers. In risk assessment studies, the Monin-Obukhov length is generally not known and must be assumed. An approach is to specify a Pasquill class to determine the Monin-Obukhov length (van den Bosch, 1997). The inlet profile is logarithmic and can be written as:

$$U(z) = \frac{u_*}{\kappa}\left(\ln\left(\frac{z}{z_0}\right) - \psi_m\right) \tag{9}$$

where the friction velocity u_* is given by:

$$u_* = \frac{U_0 \kappa}{\ln\left(\frac{z_{ref}}{z_0}\right) - \psi_m} \tag{10}$$

where U_0 is the velocity at the reference height z_{ref}. The constant ψ_m is given by van den Bosch (1997):

$$\psi_m = \begin{cases} 2\ln\left(\frac{1+\xi}{2}\right) + \ln\left(\frac{1+\xi^2}{2}\right) - 2\arctan(\xi) + \frac{\pi}{2} & \text{for } L < 0 \\ -17\left(1 - \exp\left(-0.29\frac{z}{L}\right)\right) & \text{for } L > 0 \end{cases} \tag{11}$$

where $\xi = (1 - 16z/L)^{1/4}$.

The temperature profile is given as follows:

$$T(z) = T_g + \frac{T_*}{\kappa}\left(\ln\left(\frac{z}{z_0}\right) - \psi_H\right) - \Gamma_d z \tag{12}$$

where $\Gamma_d = 0.011$ km^{-1} is the dry adiabatic lapse rate and ψ_H is given as follows:

$$\psi_H = \begin{cases} 2\ln\left(\frac{1+\xi^2}{2}\right) & \text{for } L < 0 \\ -5\frac{z}{L} & \text{for } L > 0 \end{cases} \tag{13}$$

Turbulence profiles at the inlet follow the suggestions of Han *et al.*, (2000) and depend on atmospheric stability. Expressions for turbulent profiles are not given here for simplicity; the interested reader can find them in Han *et al.*, (2000).

When performing the FLACS modeling work it is very important to strictly follow the validation based guidelines. For this particular work, this includes:

- representing the geometry layout as accurately as possible
- using correct scenario parameters (atmospheric boundary conditions, source terms)
- choosing an appropriate grid according to model guidelines
- extracting model predictions in the same way that was done during experiments

In the present simulations, the geometry models are defined in a manner as described in the Model Validation Database, with additional information obtained from the literature as required. While the geometry models should be consistent with those found in experiments, some smaller inaccuracies might still exist because the exact terrain information may not be available for some of the field tests. For example, when modeling the Burro tests, we included 2 buildings upwind of the release in the modeling and also defined the spill location 1.5m below the terrain (information found in Koopman *et al*., 1982a). On the other hand, we did not attempt to model the slightly uneven terrain downwind of the spill due to lack of detailed documentation.

With regards to the boundary conditions, the wind, turbulent kinetic energy and turbulent dissipation rate were set at the inflow (and parallel to wind) boundaries. A passive outflow condition at ambient pressure was used at the exit boundaries. A no-slip condition at the ground was specified. The wind direction, wind speed at a given reference height, Pasquill class, roughness length and ambient temperature were in general set accordingly to the Model Validation Database for each field test. In the simulations of the wind-tunnel scenarios this approach is not used because the turbulent length scales would be set too large relative to the grid cell sizes used. We instead used a logarithmic inflow wind profile with 5-10% turbulence intensity and a turbulent length scale 1-2 times the smallest grid cell size dimension.

While there should be limited room for user variability in the definition of geometry and scenario parameters when setting up the FLACS simulation model, there may be some potential for user dependency when defining the simulation mesh. Since a single-block Cartesian grid is employed, the choices for users are limited. To help users, and limit variability in simulations, validation based guidelines for grid generation exist. For the present study the most relevant guidelines are:

- The distance to domain boundaries should be large enough not to influence physics studied. If in doubt, repeat simulations with a larger domain and ensure reported results do not change.
- Expected gradients (e.g. dense gas layer) and important geometry objects (e.g. fences) should be properly resolved, whereas less critical geometry elements will be handled automatically with sub-grid porosity models. Release sources must be properly resolved, for LNG pools there should be 10 grid cells or more across the pool diameter, for diffusive gas sources at least 3-5 grid cells, and for high pressure releases maximum grid cell area should be 1-2 times the area of the jet (expanded to ambient pressure)

- Grid aspect ratios ($\Delta X/\Delta Y$) should be not more than 1:5 near the source or where velocity gradients are the highest. Grid sizes and aspects ratios can be increased further away from the source where flow and concentration gradients are less, but aspect ratio as high as 1:100 should be avoided. When stretching the grid, stretch factors ($\Delta X_{n+1}/(\Delta X_n)$) should be less than 1.2, except for local refinement near high-pressure jets where factor 1.4 is considered acceptable.
- Due to current limitation in turbulence model settings, grid cell sizes of less than 1cm may give unphysical results. If grid cell sizes of less than 1cm are used, a sensitivity study should be performed to ensure results are not impaired. This limitation was the reason for modeling some of the wind-tunnel experiments at full-scale.
- When simulating dense gas dispersion with sensors located near the ground, the grid must be made fine enough (i.e. first layer of grid cells should be below the sensor)

For most tests the exact sensor locations found in the Model Validation Database have been applied, and we have performed point-wise or arc-wise comparisons. For some wind-tunnel tests (BA-Hamburg circular fence) it was not clear whether sensor points along axis or arcs were used, here it was decided to use arcs based on the shape of the plumes observed in simulations. For large-scale field trials, wind meandering is a critical parameter when experimental observations and numerical predictions of gas concentrations are compared at a specific position. In FLACS, two time scales, typically of order 10 and 60 seconds can be set and sinusoid-shaped variations of the wind direction and wind speed are obtained at the inlet boundaries (Hanna *et al*., 2004). For Burro, Coyote and Falcon tests, where the distance between adjacent gas sensors in an arc could be significant, it was decided to use meandering wind assumption in the modeling to make sure the gas plumes would hit the sensor arcs. For Maplin Sands simulations sensor positions were instead defined along the given wind direction, so there was no need to apply the meandering wind. In the Maplin Sands experiments, the gas plumes seem to have missed many sensor arcs, and thus are not reported from the experiments and not part of the Model Validation Database.

MEP Validation

A brief summary of the MEP Database is provided next. The trials and test cases that comprise the database are shown in Table 1.

Table 1: Trials and test cases in the Database

Name	Sheet No.	Trial No.	Field (F) or Wind tunnel (WT)	Obstructed (O) or unobstructed (U)	Atmospheric stability class	Substance released	Dispersion over water (W) or land (L)
Maplin Sands 1980[a]	1	27	F	U	C-D	LNG	W
	2	34			D		
	3	35			D		
Burro, 1980[b]	4	3	F	U	B	LNG	L
	5	7			D		
	6	8			E		
	7	9			D		
Coyote, 1981[c]	8	3	F	U	B-C	LNG	L
	9	5			C-D		
	10	6			D		
Falcon, 1987[d]	11	1	F	O	G	LNG	L
	12	3			D		
	13	4			D-E		
Thorney Island 1982-4[e]	14	45	F	U	E-F	Freon 12 & Nitrogen	L
	15	47			F		
CHRC, 2006[f]	16	A	WT	U	D	Carbon Dioxide	L
	17	B		O	D		
	18	C		O	D		
BA-Hamburg[g]	19	Unobstructed (DA0120)	WT	U	D	Sulfur Hexafluoride	L
	20	Unobstructed (DAT223)		U	D		
	21	Upwind fence (039051)		O	D		
	22	Upwind fence (039072)		O	D		
	23	Downwind fence (DA0501)		O	D		
	24	Downwind fence (DA0532)		O	D		
	25	Circular fence (039094/039095)		O	D		
	26	Circular fence (039097)		O	D		
	27	Slope (DAT647)		U	D		
	28	Slope (DAT631)		U	D		
	29	Slope (DAT632)		U	D		
	30	Slope (DAT637)		U	D		
BA-TNO[h]	31	TUV01	WT	U	D	Sulfur Hexafluoride	L
	32	TUV02		O	D		
	33	FLS		U	D		

a MDA (Hanna *et al.*, 1991). Also data reports (Colenbrander *et al.*, 1984a,b,c), Ermak *et al.* (1988).
b REDIPHEM (Nielsen & Ott, 1996). Also MDA, Burro data report (Koopman *et al.*, 1982a,b) and Ermak *et al.* (1988).
c REDIPHEM. Also MDA, Coyote data report (Goldwire *et al.*, 1983), Morgan *et al.* (1984), and Ermak *et al.* (1988).
d Data report (Brown *et al.*, 1990)
e MDA. Also see Ermak *et al.* (1988).
f Havens & Spicer (2005, 2006, 2007) & CHRC – University of Arkansas.
g REDIPHEM. Also see Schatzmann *et al.* (1991), Nielsen & Ott (1996).
h REDIPHEM. Also see Nielsen & Ott (1996).

For more detailed information the reader is referred to the *Guide to the LNG Model Validation Database* (Coldrick *et al*., 2009). The Database is contained in a Microsoft Excel workbook. The details of the test conditions are provided in each worksheet, together with concentration measurements and, for some tests, temperature measurements. For the wind tunnel tests, measurements are provided at wind tunnel scale and full-scale, so the modeler can choose whether to model wind tunnel test or the scaled-up scenario. Each worksheet contains an area for model output data to be added where the results of the FLACS simulations were input. The completed database can be downloaded from the GexCon US website (www.gexconus.com).

There are many experimentally-measured physical comparison parameters in the Database and include: maximum concentration along an arc at a given distance from the source, cloud width along an arc at a given distance from the source, concentrations at specific sensor locations, and for certain experiments the point-wise temperature is provided. Both "short" and "long" averaging times are provided for physical comparison parameters for some tests. To avoid zero division when evaluating statistical performance measures a threshold value of 0.1% of the vapor concentration has been applied to the database, where all values below this value are omitted from the database, and any model prediction lower than this threshold value will be given the value 0.1%.

For all of the wind tunnel tests and the Thorney Island field trials, the source term is well-defined as a constant flux of vapor over a specified area. Therefore, no source term model is required for these tests. For the Maplin Sands, Burro, Coyote and Falcon field trials the LNG is spilled onto a large water pool, and in all except the Maplin Sands test cases, a splash plate was present to direct the LNG laterally across the surface of water. Unfortunately, little accurate information exists on the size of the spreading LNG pools. A source model is required for these field tests.

The final two sheets of the database provide tabulations of the statistical performance measures (SPM): mean relative bias, mean relative square error, the fraction of predictions which are within a factor of two of the measurements, geometric mean bias, and geometric variance. The SPM are computed over all test cases in the sheet, but are split into two groups. Group 1 contains the unobstructed tests and Group 2 the obstructed tests:

- Group 1: Maplin Sands, Burro, Coyote, Thorney Island, CHRC Case A, BA-Hamburg unobstructed and slopes, BA-TNO unobstructed & FLS (highlighted blue in Table 1)
- Group 2: Falcon, CHRC Cases B & C, BA-Hamburg cases with fence, BA-TNO with fence (not highlighted in Table 1).

In the following sections, most of the descriptions regarding the experimental setups and associated images were taken from Coldrick *et al*. (2009).

Group 1: MEP Unobstructed Database

Maplin Sands Tests 27, 34, and 35

The Maplin Sands trials were conducted by Shell Research limited in 1980 and consisted of 34 spills of liquefied gases onto the sea (Colenbrander *et al*., 1984a,b,c). Both continuous and instantaneous releases of propane and LNG were carried out. The release site was an area of

tidal sands in the Thames estuary and is shown in Figure 2. The spill point was a 150mm diameter pipe directed vertically downward terminating above the water surface. The termination point varied for each experiment. No "splash plate" was used below the pipe exit.

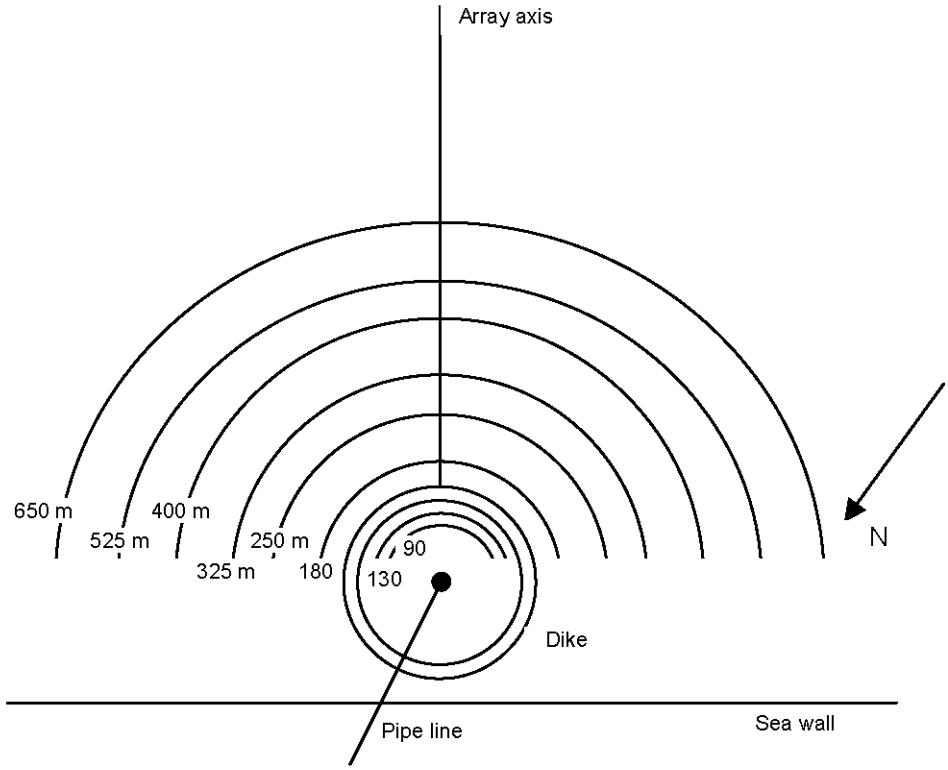

Figure 2: Maplin Sands spill area

Instruments were set in arcs surrounding the spill point. Experimental results were obtained at the specified sensors and steady-state arc concentrations for the natural gas are reported. The FLACS model setup was as specified in the MEP along with addition information from Hanna *et al*. (1991) and the summary report by Ermak *et al*. (1988). The LNG spill model was used to compute the spread and vaporization of the LNG on water. The sea was modeled as a flat surface and the wind was assumed along the "Y" axis as shown below.

The following wind and release characteristics were reported and used for the simulations:

Maplin Sands Test 27:	23.2 kg/s release for 160s with 5.5 m/s wind speed
Maplin Sands Test 34:	21.5 kg/s release for 95s with 8.6 m/s wind speed
Maplin Sands Test 27:	27.1 kg/s release for 135s with 9.8 m/s wind speed

The choice of grid for the simulations was: domain (X:-300 to 300m, Y: -300 to 900m, Z: -0.33 to 100m) and the grid resolution for the near field was 1m x 1m x 0.33m. Typical simulation times were approximately 4 CPU-days. The predicted plumes as well as comparison to experiments can be seen in Figure 3. For the Maplin Sands trials the FLACS simulation results were good and compared well with the experimental data.

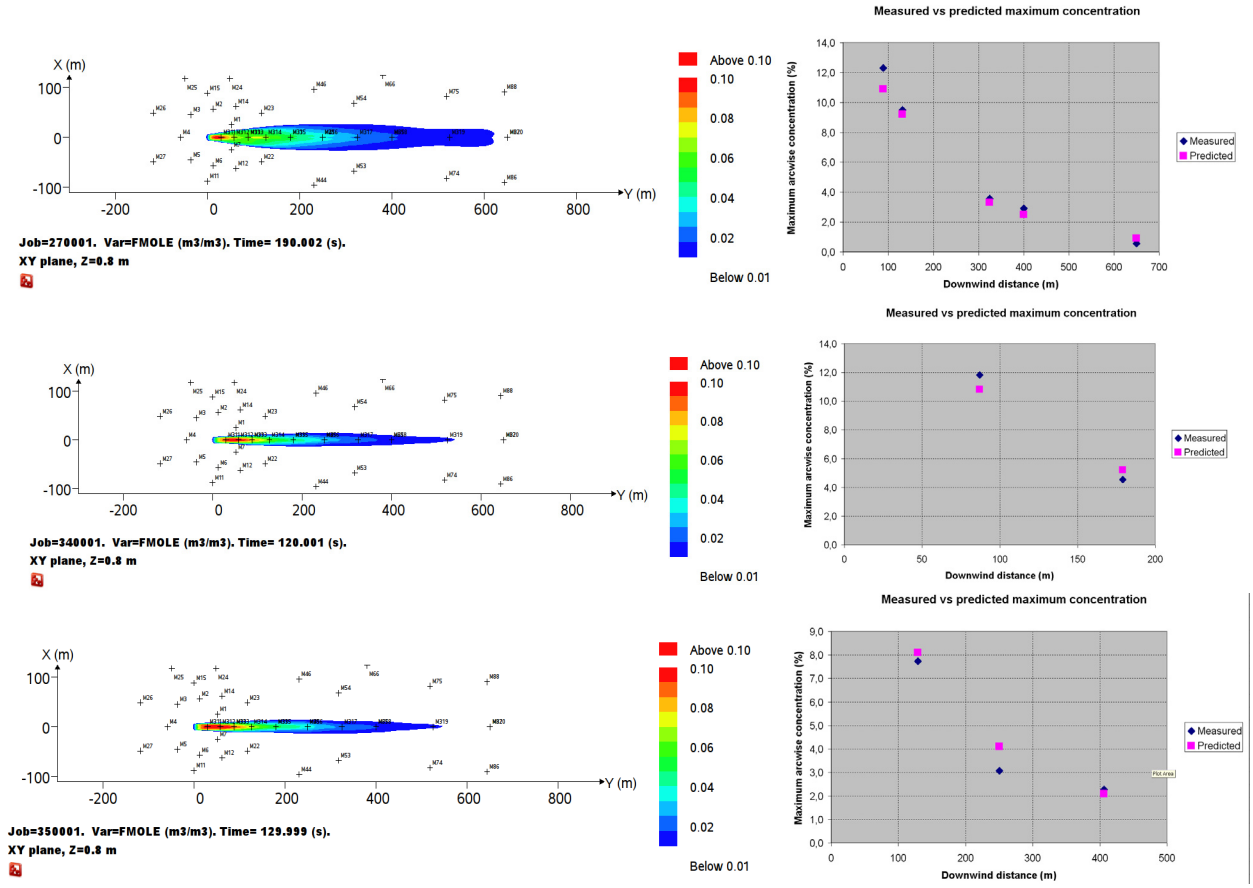

Figure 3: Steady state plumes (left) and measured versus predicted concentrations (right) for MS 27 (top), MS 34 (middle) and MS 35 (bottom)

Burro Tests 3, 7, 8, and 9

The Burro series of experiments (see Koopman *et al*., 1982b) were performed at the Naval Weapons Center, China Lake, California in the summer of 1980. There were eight LNG spills between 24m^3 and 39m^3 onto water. A complete description of the test site and spill area can be found in Koopman *et al*. (1982b) and Goldwire *et al*. (1983) and is shown schematically in Figure 4. A 25 cm diameter spill line terminated 1.0 m above the surface of the water basin and a splash plate was fitted below this pipe outlet to limit penetration of the LNG into the water. The splash plate was located just below the water surface to direct the flow of LNG horizontally across the water. The water test basin had an average diameter of 58m and a water depth of 1m. The water level was approximately 1.5m below the ground level. The terrain downwind of the spill pond sloped upward at about 7 degrees for 80m, before leveling out to about a 1-degree slope.

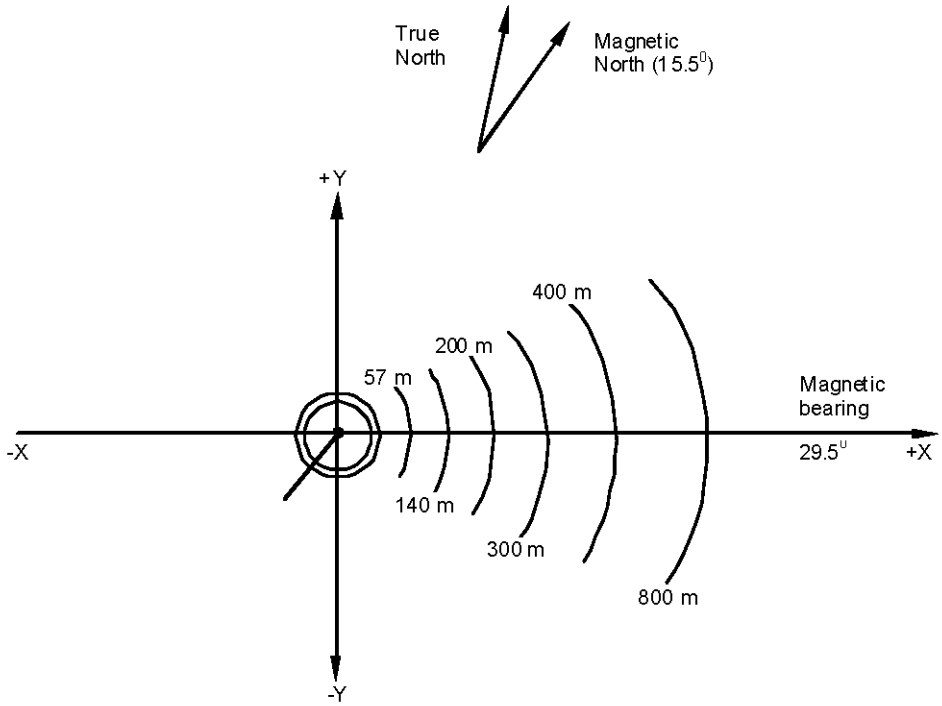

Figure 4: Burro and Coyote spill area

Instrumentation was placed at gas measurement stations located at arcs downwind from the spill point at 57, 140, 400 and 800 m. The array centerline was orientated at 225 degrees, from the southwest, to coincide with the prevailing winds. Data was reported in short- and long-time averaging of pointwise and arc locations as well as plume width. Average wind data was provided.

The experiments were simulated using the LNG spill and pool spread model. The ground was modeled as flat surface. The spill pond was defined 1.5m below ground level, and 2 upwind buildings were included as objects in the modeling. For all tests the wind speed provided in the database was used for the modeling. For most conditions this may be a good assumption, however, in the Burro 8 tests very significant changes in wind were observed during the experiments and it is not obvious how to choose a representative wind condition. The reported test conditions that were used for the modeling were:

Burro Test 3: 88 kg/s release for 167s with 5.6 m/s wind speed
Burro Test 7: 99 kg/s release for 174s with 8.8 m/s wind speed
Burro Test 8: 117 kg/s release for 107s with 1.8 m/s wind speed
Burro Test 9: 136 kg/s release for 79s with 5.9 m/s wind speed

Because a scattered array of sensors was used in the experiments, a narrow vapor plume may at times pass through a sensor arc without hitting any sensors. During the experiments, atmospheric wind direction changes ensured that near maximum plume concentrations were recorded at sensors of all the arcs. To make sure this would also happen in the simulations, a meandering wind field was used in the simulations in which moderate velocity and directional changes were

made to the inflow wind field during the simulation (see Hanna *et al*., 2004). The atmospheric stability class B was reported for test 3, however, modeled in FLACS as class D per GexCon user recommendations. The choice of grid for the simulations was: domain (X:-100 to 600m to 900m, Y: -200 to 200m, Z: -2 to 50m) and the grid resolution for the near field was 1m x 1m x 0.5m. Typical simulation times were approximately 3 CPU-days.

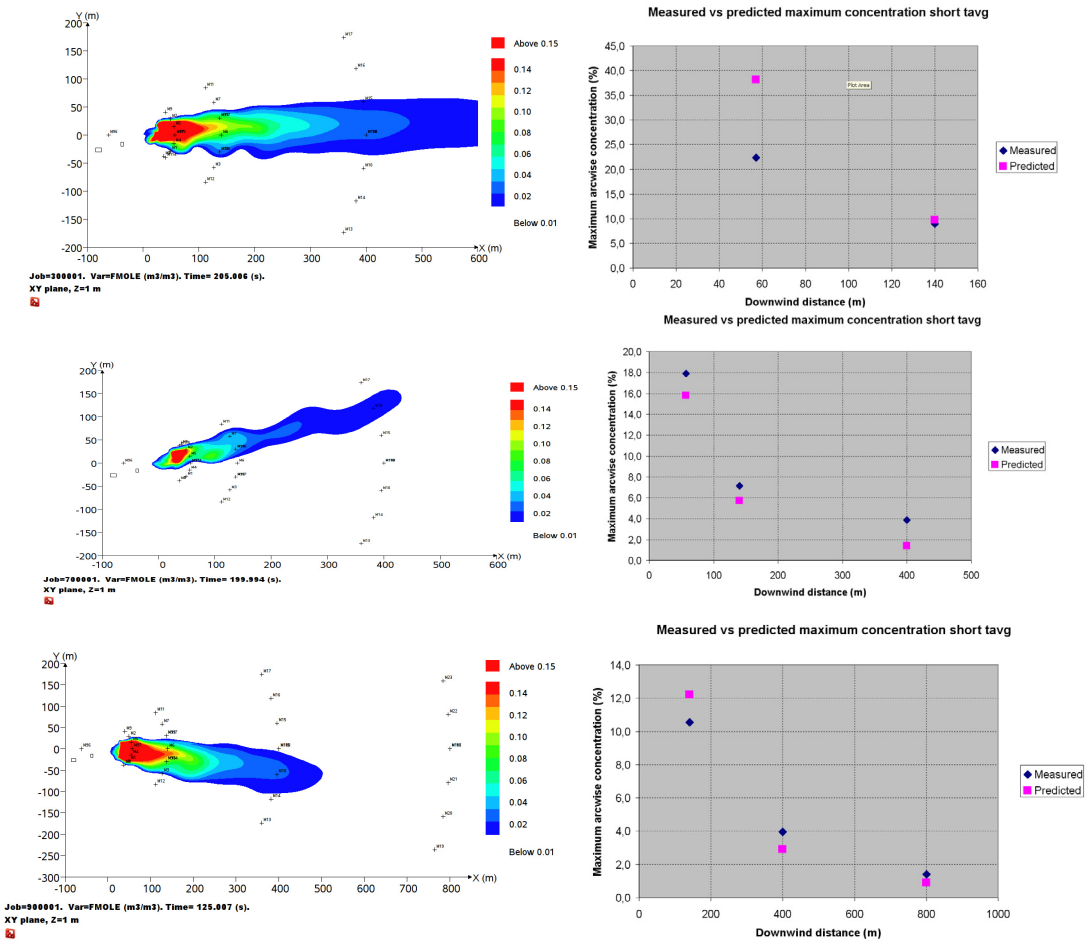

Figure 5: FLACS simulations (left) and comparison with experiments (right) for Burro tests 3 (top), 7 (middle) and 9 (bottom)

FLACS simulations were generally good for most of the experimental data in Burro tests 3, 7 and 9, and are shown in Figure 5. Some results were over-predicted for the long time average and point-wise concentrations. These results would improve with a more accurate representation of the observed wind-fields, as the wind fluctuations during the experiments were generally stronger than assumed in our modeling.

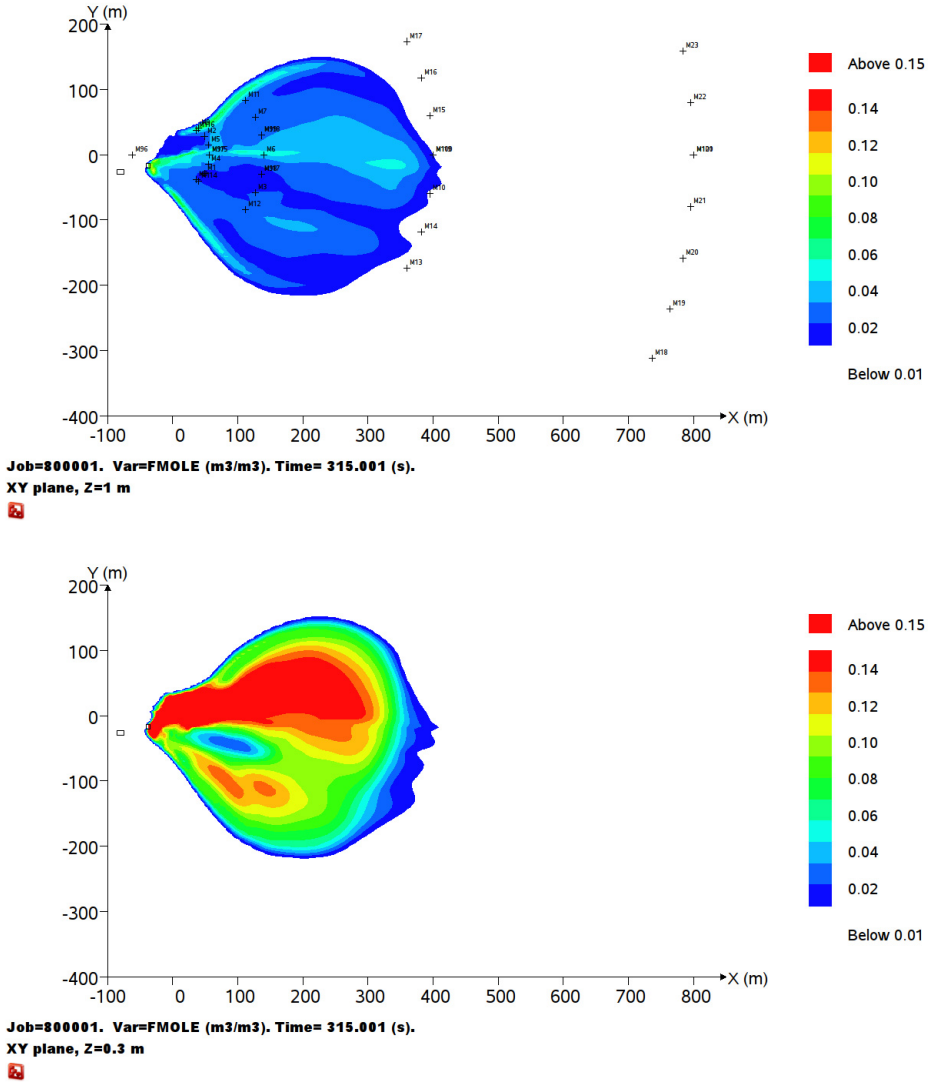

Figure 6: FLACS Simulations for Burro test 8 at 1m height (top) and 0.3m (bottom)

One notable disagreement occurred for the Burro test 8 at the sensor locations that were reported 1m above the ground. This test case had very little wind and the FLACS results at 1m under-predicted the experimental results for the first two sensor arcs (57m and 140m), but predicted well concentrations at 400m and 800m arcs as well as distance to ½ LFL and LFL. There are various possible reasons for the under-prediction, e.g. uneven terrain not accounted for in simulations which makes gas reach lower lying sensors in the terrain, higher atmospheric wind variation than assumed in the modeling, or a stronger source turbulence in the pool than assumed. In the simulations concentrations consistent with the 1m sensor recordings were observed at 0.3m above the ground, showing the very dense "pancake" shape of the plume as shown in Figure 6. The influence of terrain on the transport of dense gas cloud has been identified by several authors (see e.g. Koopman *et al*., 2007)

Coyote Tests 3, 5 and 6

The Coyote series (see Goldwire *et al*., 1983) followed a similar format and setup as the Burro tests and were intended for the study of vapor burn and Rapid Phase Transition (RPT) explosions that had been observed in the Burro trials. The Coyote trials consisted of five vapor dispersion and burn experiments and five experiments for investigation of RPT occurrences. Spill volumes were between 3.3 and 28 m^3. One difference for the Coyote series of tests is that the sensors were concentrated closer to the spill location, and thus most sensors were relocated to the 140m and 400m arcs (see Figure 4).

Similar to the Burro test series, the experiments were simulated using the LNG spill and pool spread model, with the ground modeled as a flat surface and the spill pond 1.5m lower than the ground level. The wind speed was modeled as provided in the database, again with assumed periodic meandering to ensure that simulated plume would hit sensor arrays. Tests 3 and 5 with atmospheric stability classes B/C were modeled in FLACS as class D per GexCon user recommendations. The choice of grid for the simulations was: domain (X:-100 to 600m, Y: -200 to 200m, Z: -2 to 50m) and the grid resolution for the near field was 1m x 1m x 0.5m. Typical simulation times were approximately 3 CPU-days. The reported release and wind speed characteristics for each test were:

Coyote Test 3: 101 kg/s release for 65s with 6.8 m/s wind speed
Coyote Test 5: 129 kg/s release for 98s with 10.5 m/s wind speed
Coyote Test 6: 123 kg/s release for 82s with 5.0 m/s wind speed

FLACS simulations were generally good for most of the experimental data in Coyote 3, 5 and 6 and are shown in Figure 7. Some results were over-predicted for the long time average and point-wise concentrations, these deviations were expected due to the wind variations observed during the experiments and would likely be improved if the actual wind fluctuations had been modeled.

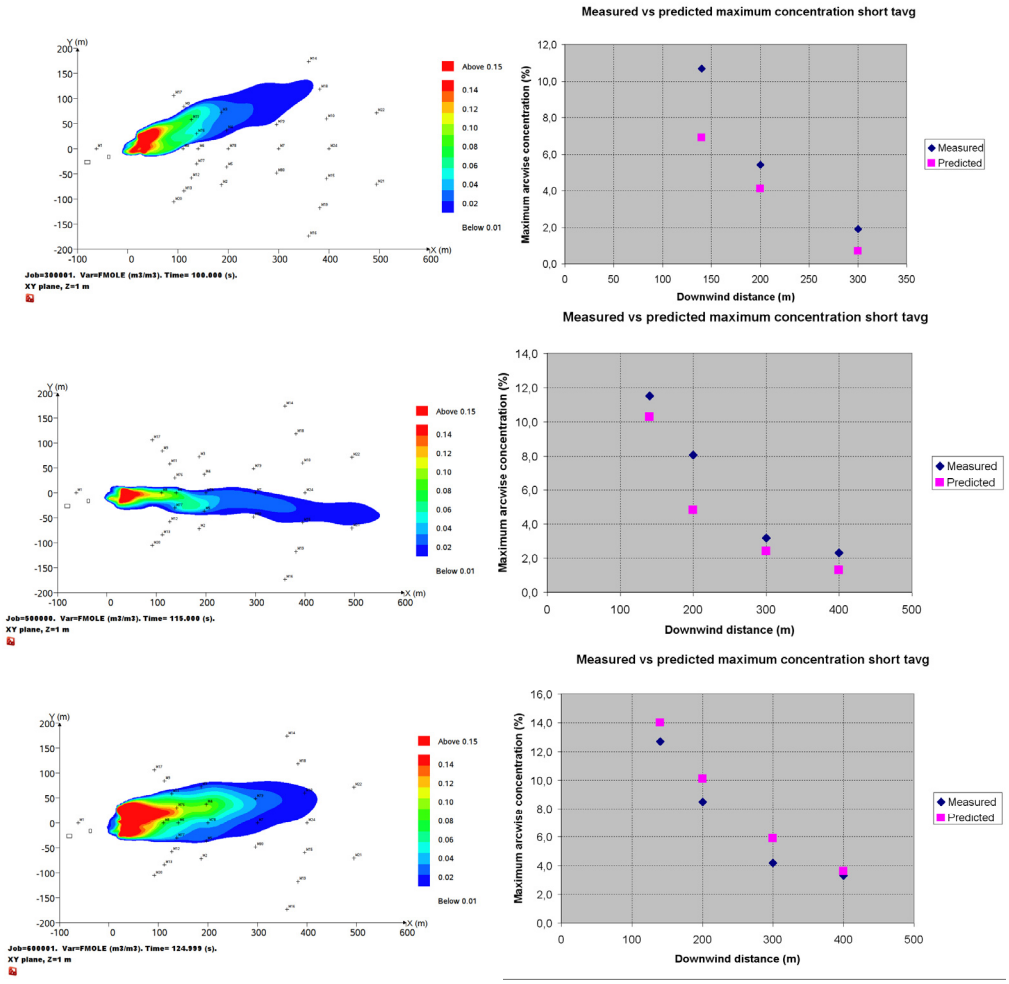

Figure 7: FLACS Simulations (left) and comparisons to experiment (right) for Coyote Tests 3 (top), 5 (middle) and 6 (bottom)

Thorney Island Tests 45 and 47

The Heavy Gas Dispersion Trials at Thorney Island were set up by the British Health and Safety Executive for the study of the dispersion of fixed volume releases of heavy gas (a mixture of Freon12 and Nitrogen, see McQuaid, 1987). Tests 45 and 47 were continuous release trials. The test site was a former Royal Air Force station at Thorney Island. The test area was largely clear for a length of 2 km and a width of 500 m and flat to within 1 in 100. The release position consisted of a vertical duct emerging at ground level underneath a 2 m diameter cap situated 0.5 m above the ground. This arrangement was designed to release the gas with near-zero vertical momentum. The spill area is schematically shown in Figure 8.

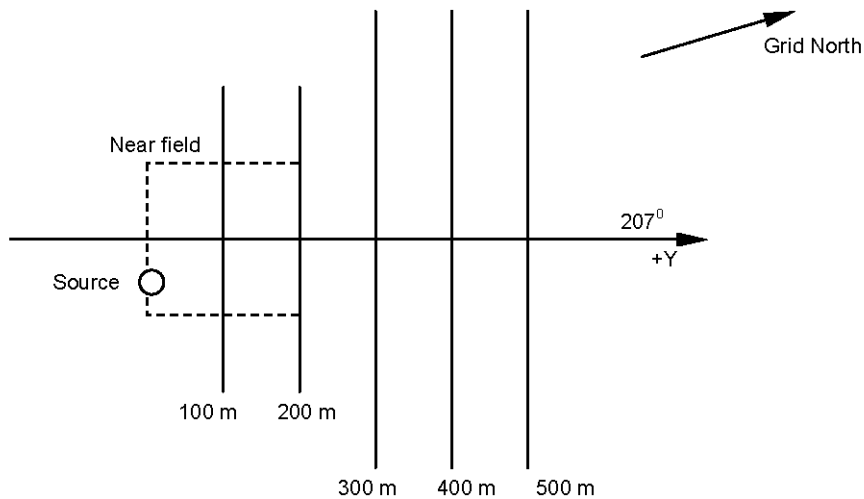

Figure 8: Thorney Island spill area

The instrumentation was largely mounted on 38 fixed towers, each with five gas sensors. The sensors in the far field (greater than 250 m) were disposed at approximately 100m intervals on a uniform grid, while a more concentrated array was used in the near field. In the model validation Database (Coldrick *et al*., 2009) no information was provided about the elevation of the lower sensors. However, other sources have reported 0.4m as the elevation of the lower sensors (Hanna *et al*. 1991).

For the present simulations the source was released via a 1m-diameter pipe, impinging on a 2m-diameter vertical plate located 0.5m above. Flat terrain was assumed in the modeling as well as steady wind direction. The choice of grid for the simulations was: domain (X:-300 to 100m, Y: -50 to 500m, Z: -1 to 25m) and the grid resolution for the near field was 0.8m x 0.8m x 0.25m. The resulting grid was 250,000 cells, with a 6h simulation time. Note: upwind distance should be increased for Y-direction for test 47 as the dense cloud migrates against the wind and the grid should be stretched less for optimal results. The wind speed and release rates reported and used are:

Thorney Island Test 45:	Release rate 10.7 kg/s for 455s in 2.3 m/s wind field
Thorney Island Test 47:	Release rate 10.2 kg/s for 465s in 1.5 m/s wind field

FLACS simulations were generally good in the far field; however, near field experimental data was significantly under-predicted by simulations as the predicted gas cloud was mainly below the sensor array at 0.4m elevation (model predictions at 0.1m compared better to near field observations). Uneven or slightly sloping ground could justify using concentrations at locations below 0.4m and could possible account for differences in the experimental data and predictions. Figure 9 and Figure 10 show the data at 0.1m and 0.4m for test 45 and for test 47.

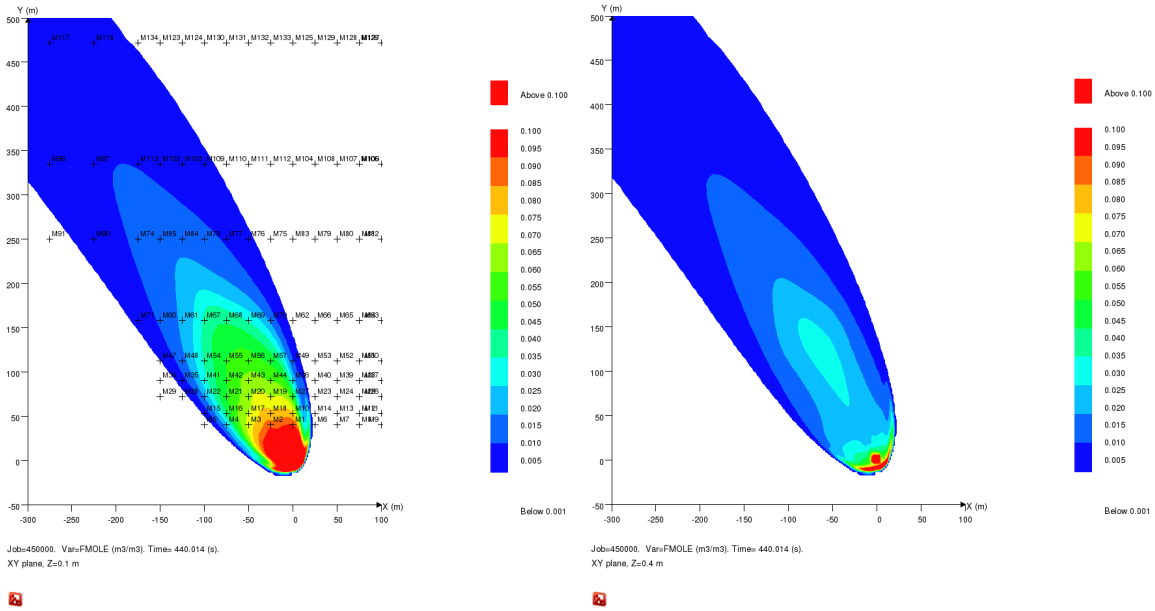

Figure 9: FLACS simulations for Thorney Island test 45 at 0.1m (left) and 0.4m (right)

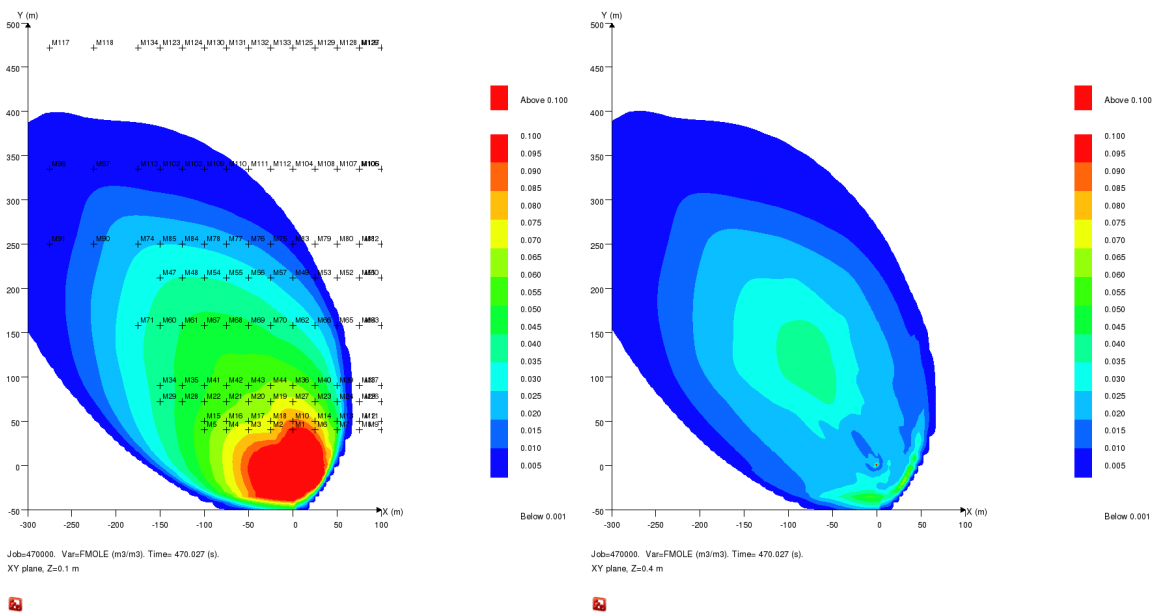

Figure 10: FLACS simulations for Thorney Island test 47 at 0.1m (left) and 0.4m (right)

One notable comment is that the initial "plow shaped plumes" observed in the FLACS simulations were able to reconcile an unexplained observation by Ermak *et al*. (1988) where they found that the plume was moving 30-50m along instrument array before turning 30 degrees with the prevailing wind, see statements from their report below:

> (2) The pattern of gas concentration data suggests that the cloud moved along the axis of the instrument array (0°) for about 30 to 50 m before it turned to the left and moved along the general direction of the wind vector (-32.6°). This initial movement was slightly uphill; the subsequent cloud track along the wind vector was slightly downhill.

CHRC Test A

The Chemical Hazards Research Center at the University of Arkansas carried out wind tunnel experiments of the dispersion of CO_2 over rough surfaces, with and without obstacles (Havens and Spicer, 2005, 2006, 2007). The floor was artificially roughened to give turbulence properties similar to field-scale. The experiments were at a scale of 1:150 of real scale and consisted of the following three cases:

Case A: Low-momentum area source CO_2 release without obstacles.
Case B: Low-momentum area source CO_2 release with tank and dike.
Case C: Low-momentum area source CO_2 release with dike only.

Results for Case A will be discussed here and the other two in the next section Group 2. The wind tunnel was an ultra low-speed boundary layer wind tunnel able to simulate the constant stress layer of the atmospheric boundary layer. Airflow from the driving fans passes through a circular-to-rectangular transition to a 7 x 20 x 80 ft (2.1 x 6.1 x 24.4 m) working area in which the floor was covered with smooth rubber matting on which roughness elements were mounted.

A 1:150 model of the tank and dike was installed on the floor (see Figure 11). The dike was square with an inner dimension of 63 cm and a wall height of 3.7 cm. The model tank was 31cm in diameter with a spherical dome top and an overall height of 28.3 cm. The tank was located in the center of the dike on a mesh screen through which the gas flowed. The area through which gas is released is identical in all three release cases – A, B and C, at 0.3341 m^2 (Havens, 2007). That is, gas enters through a square-shaped area with a central circular section blanked-off. The gas was CO_2 released at room temperature at a rate of 33.4 liters/minute, with 0.5 liters/minute of propane added - as a tracer. The wind speed was 0.4 m/s at a reference height of 6.7 cm. Gas concentration measurements were made at an elevation of 0.5 cm and in 10 cm lateral intervals across the cloud. Long-time averages of the data are given. In addition to the gas concentration, measurements were made of the upwind approach flow mean velocity profile.

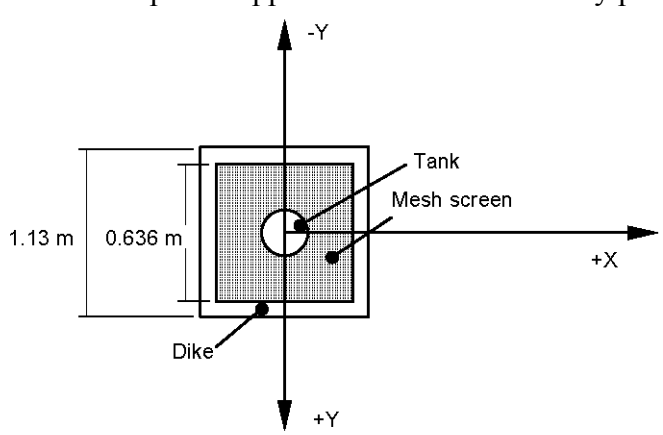

Figure 11: CHRC source layout

FLACS simulations were conducted using a 3 x 3 diffusive leak underground in a rectangular hole. Above the leak there is a grid with 50% porosity vertically (no lateral porosity) to ensure a reasonably steady and even flow up from the defined leak source area. Sensors were

implemented at specified locations. Flat ground was modeled along with 3 x 3cm roughness elements defined. Wind profile was defined with 5% turbulence intensity and 3mm length scale, which is equal to the minimum grid cell size. The choice of grid for the simulations was: domain (X:-1 to 6m, Y: -1.5 to 1.5m, Z: -0.02 to 1m) and the grid resolution for the near field was 30mm x 30mm x 3mm. This resulted in 220,000 grid cells, and typical simulation times were approximately 2 CPU-days. FLACS grid guidelines recommend that minimum grid cell size should be at least 10mm and aspect ratio less than 5. The reasons for deviating from the guidelines were the need for vertical resolution around the sensor location only 0.5cm above ground and resolve the dike height of 3.7cm sufficiently. Alternatively, if we were to strictly follow the grid guidelines we would have to model the 150:1 scaled-up scenario instead. For quality check, comparable results were obtained with a coarser grid using 10mm in the vertical direction and 15h CPU time.

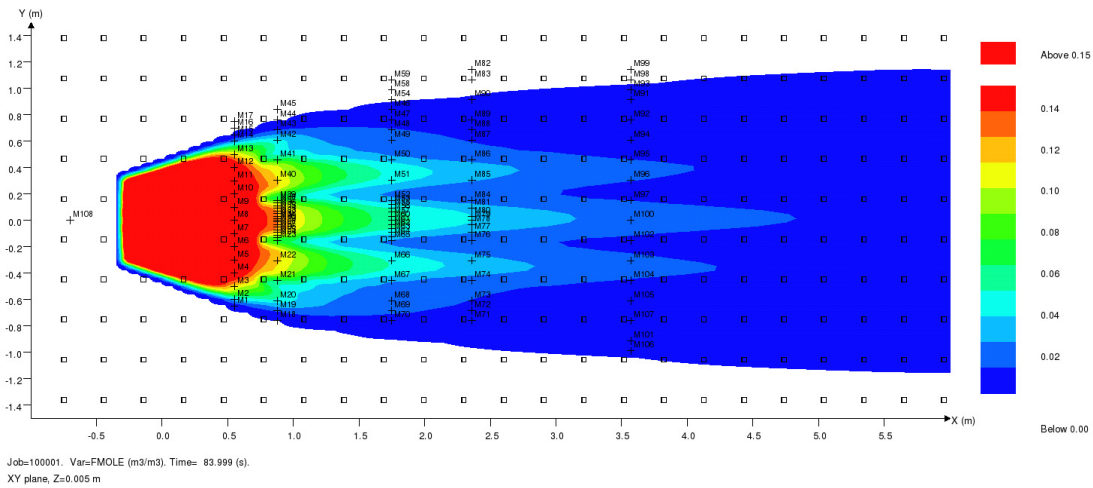

Figure 12: FLACS simulations of the plume for CHRC case A

Results from the FLACS simulations were in very good agreement with experimental data. Figure 12 shows the plume for case A. It should be noted that the 3 x 3 diffusive leak used might have an influence on the observed triple tailed plume; however, this was also observed for the dike case (discussed later).

BA-Hamburg tests

The BA-Hamburg trials were conducted in an open circuit wind tunnel at the Meteorological Institute at the University of Hamburg and are all continuous releases of sufficient duration that stable statistics were obtained (Nielsen & Ott, 1996). The University of Hamburg wind tunnel is 16 m long and consists of an inlet nozzle with flow straighteners, a 7.5 m long establishment section, a 4 m long test section, and finally a centrifugal fan. The width and height of the test section are 1.5 m and 1 m, respectively. The tunnel is suction-driven to keep disturbances in the tunnel to a minimum. An adjustable ceiling is used to establish a zeropressure- gradient boundary layer. Irwin spires are followed by distributed roughness elements (2 cm high Lego blocks) in the establishment section to provide a turbulent boundary layer profile. The trials comprised floor-level area gas source releases of sulfur hexafluoride (SF_6) at room temperature. The gas was introduced into the wind tunnel through a perforated circular plate approximately 7 cm in diameter and mounted flush into the tunnel floor. The experiments were at a model scale

of 1:164. Gas concentration measurements were made at floor level using an aspirated film probe.

Tests DA0120 and DAT223

Figure 13 shows the test arrangement for the unobstructed reference cases DA0120 and DAT223.

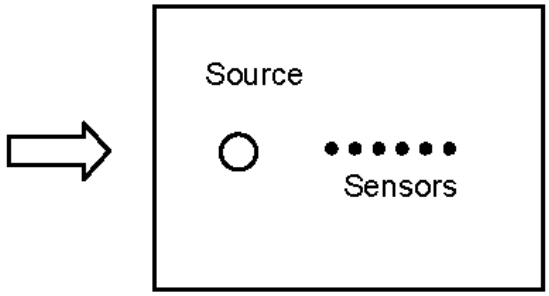

Figure 13: BA-Hamburg setup for unobstructed reference cases

FLACS simulations included the geometry as specified in the MEP, but to be able to comply with the FLACS grid guidelines the scaled-up results were used due to the small dimensions in the experiments. The source was specified as a diffusive leak from a cylindrical hole (an 11.2m diameter was inadvertently used instead of the 11.48m actual size, but this deviation was not judged serious enough to redo the calculations). A 50% porous grid was used in the vertical direction to ensure an upward distributed flow. Flat ground was assumed in the simulations and sensors were defined at ground level (5cm elevation). The wind profile was assumed with 5% turbulence intensity and length scale equal to the smallest grid resolution. The choice of grid for the simulations was: domain (X:-80 to 480m, Y: -75 to 75m, Z: -3 to 25m) and the grid resolution for the near field was 1m x 1m x 0.2m. The resulting grid was 240,000 cells, with an approximately 1-day simulation time. Arc-wise results were reported at the center axis similar to those reported in the MEP.

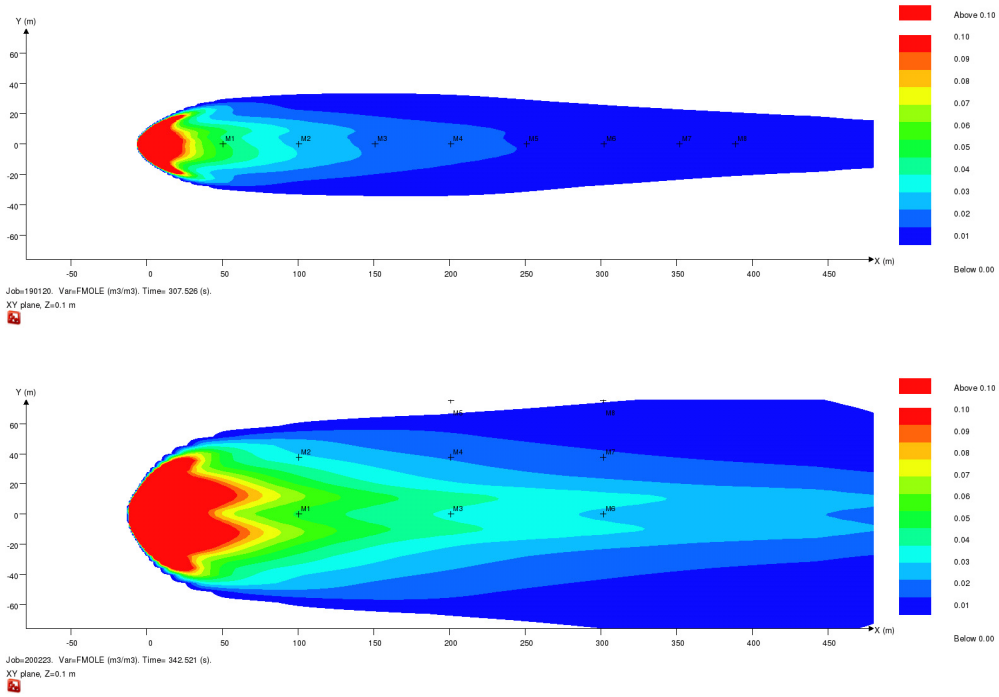

Figure 14: FLACS simulations for tests DA0120 (top, 60 kg/s SF_6 release in 6.92 m/s wind field) and DAT223 (bottom, 300 kg/s SF_6 release in 9.47 m/s wind field)

FLACS predictions were generally very good for the given data sets. Some under-prediction was observed in the near field for the first test (with the lowest release rate). These results could be potentially improved with a finer grid resolution in the vertical direction.

Tests DAT647, 631, 632, 637

Figure 15 shows the test arrangement for the unobstructed reference cases DAT647, 631, 632 and 637.

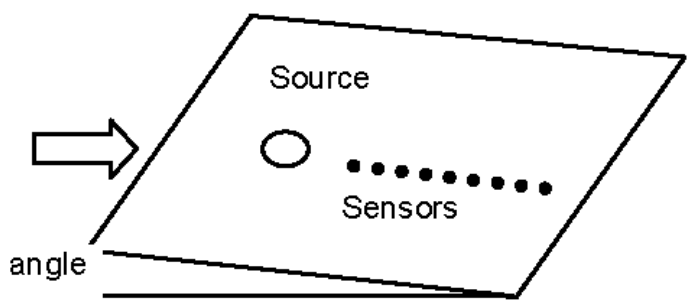

Figure 15: BA-Hamburg setup for sloping terrain

A similar setup procedure was used in this as the flat terrain cases. To account for the sloping terrain the direction of the gravity was adjusted accordingly. Again the arcwise points along the center axis were analyzed as reported in the MEP. FLACS simulations were fairly good, however, there was some deviation. The results could have been improved with a finer grid

resolution and an increased computational domain. Figure 16 shows the results for the present four cases.

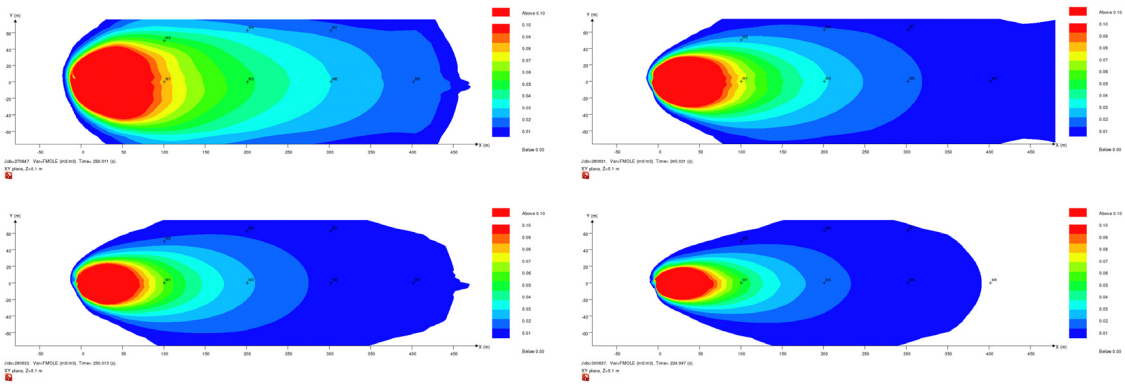

Figure 16: FLACS simulations of the BA-Hamburg tests DAT647 (upper left, 60 kg/s SF_6 release and 4% slope), 631 (upper right, 90 kg/s SF_6 release and 8.6% slope), 632 (lower left, 60 kg/s SF_6 release and 8.6% slope) and 637 (lower right,60 kg/s SF_6 release and 11.6% slope)

BA-TNO tests TUV01 and FLS

The experiments were conducted in the TNO "Pollution Industrial Aerodynamics" wind tunnel facility (Nielsen & Ott, 1996). The wind tunnel is an open, Eiffel-type wind tunnel. After the contraction an initial velocity and turbulence profiles which compare to the atmospheric profiles at a small scale (1:100 to 1: 500) are made using "shark fin" or Counihan-vortex generators and a crenellated barrier. Between the vortex generators and the actual test section is a boundary layer conditioning section of about 10m length. The test section of the wind tunnel is 6.8m long, 2.65m wide and 1.2m high, not including the upstream boundary layer conditioning section. The surface was horizontal.

The wind tunnel trials used a surface release of SF_6 at floor level. The source consisted of a 107mm diameter orifice covered in a 50% porosity gauze to give a vertical low-momentum release. The TUV01 release took place over a period of 500s, while the FLS experiment consisted of a continuous release (over 1000s) with an unobstructed 3D measurement field. The gas concentrations in the TUV01 trial were measured at floor level using aspirated hot-wire probes. Figure 17 shows a schematic of the BA-TNO trials.

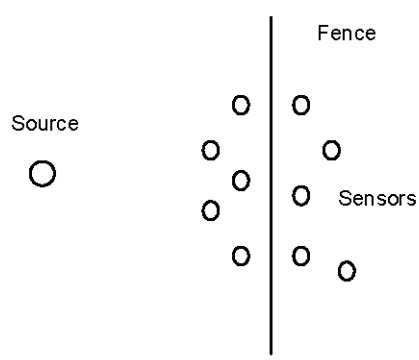

Figure 17: TNO experimental setup

FLACS simulations were implemented at 78:1 scale to comply with FLACS grid guidelines, using a diffusive leak from a cylindrical hole (8.35m diameter). A 50% porous grid in the vertical direction was used to ensure a distributed flow in the upwards direction. Flat terrain was assumed and the wind profile used a 10% turbulence intensity and a length scale of 0.2m (1-2 times the smallest grid size). Sensors were assumed to be at ground level. The choice of grid for the TUV01 simulations was: domain (X:-25 to 100m, Y: -50 to 50m, Z: -3 to 25m) and the grid resolution for the near field was 0.5m x 0.5m x 0.1m (380,000 grid cells) and for the FLS domain (X:-80 to 350m, Y: -75 to 75m, Z: -3 to 25m) and the grid resolution for the near field was 1m x 1m x 0.2m (250,000 grid cells).

Figure 18 present the FLACS simulations of the TUV01 along with measured concentrations on the graph. It is difficult to understand the experimental distribution of gas concentrations as it appears that higher concentrations were measured further downstream the source. For the FLS experiment FLACS simulations were in good agreement with the test data and are shown in Figure 19.

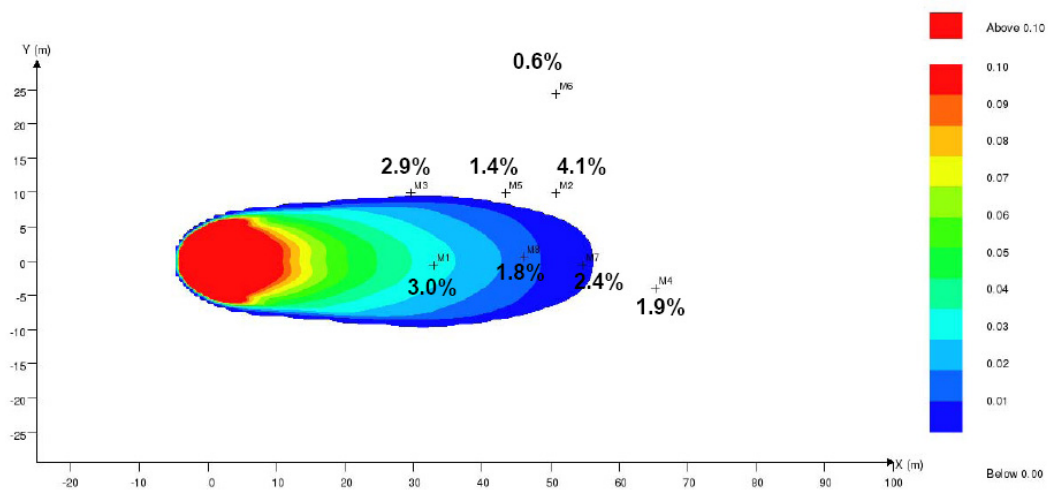

Figure 18: BA-TNO TUV01 simulations and experimental values (Scaled scenario with release rate of 13.43 kg/s SF_6 in a 5.12 m/s windfield)

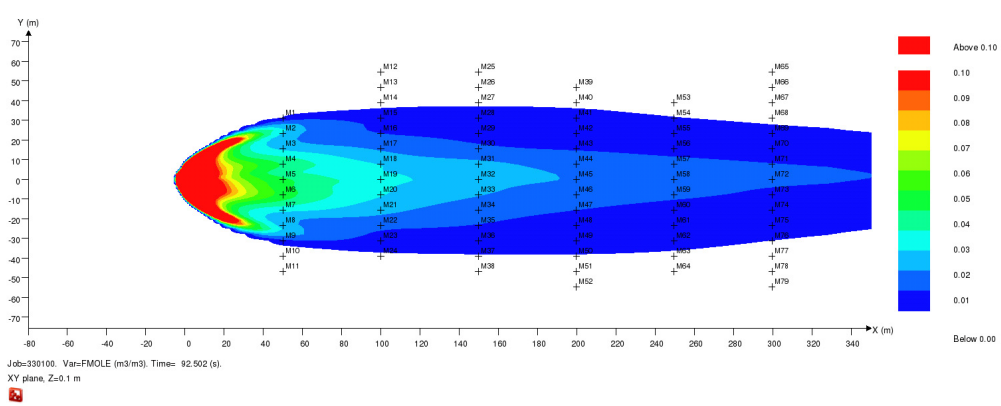

Figure 19: BA-TNO FLS FLACS simulations (Scaled scenario with release rate of 56.2 kg/s SF_6 in a 6.88 m/s windfield)

Group 2: MEP Obstructed Database

Falcon Tests 1, 3 and 4

The Falcon trials (see Brown *et al*. 1990) were a series of five large-scale LNG spill tests carried out by the Lawrence Livermore National Laboratory (LLNL). The trials were carried out at Frenchman Flat, an extremely flat playa with little vegetation. The trials had the purpose of evaluating the effectiveness of vapor fences as a mitigation technique for accidental releases as well as providing a dataset for model validation purposes. The spills (between 20 and 63 m^3 of LNG) were onto a specially designed water pond equipped with a circulating system to maximize evaporation (see Figure 20).

Figure 20: Falcon test setup – Courtesy of R.P. Koopman

The main 10” (25.4 cm) diameter spill pipe terminated immediately above the centre of the pond and then divided into 6” (15.2 cm) diameter pipes as a multi-exit “spider” to provide a uniform distribution of LNG over the spill pond. The spider consisted of four arms of 11.6 m length oriented at 90 degrees to each other as shown in Figure 21.

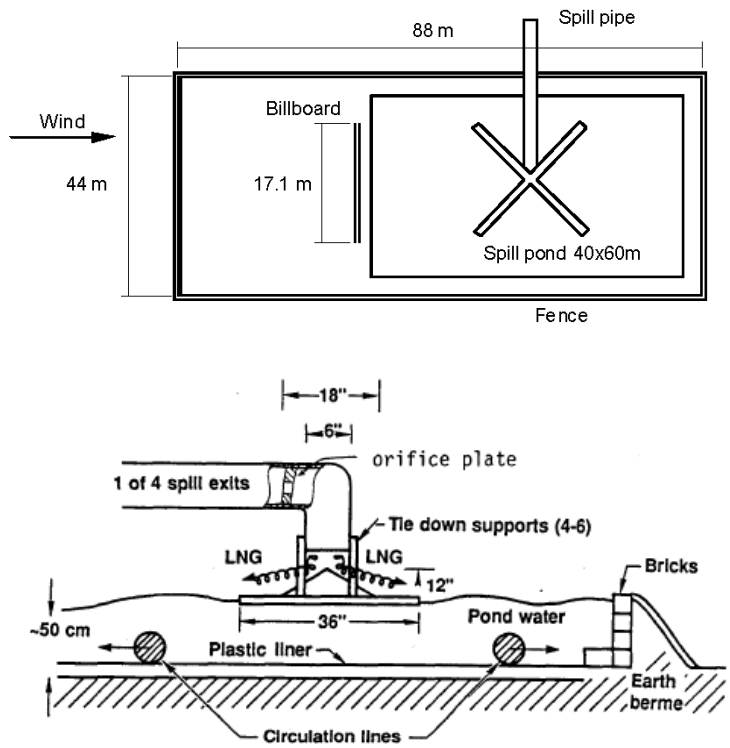

Figure 21: Falcon test setup of the "spider" above and spill exit (below)

Gas concentration and temperature sensors were arranged in three downwind station arrays at 50 m, 150 m and 250 m. Each station had sensors disposed at 1 m, 5 m, 11 m and 17 m above the ground. The layout remained largely unchanged between tests other than between Falcon 3 and 4 when two stations were moved from the 50 m row to the 150 m row. The instrument array centerline was oriented at 225 degrees, from the southwest, to coincide with the prevailing wind direction.

Three tests were included in the Model Validation Database, these were Falcon 1, 3 and 4. Falcon 5 was excluded because strong RPTs led to ignition of the vapor during the test. The following characteristics for the tests were found in the validation database and used in the modeling:

Falcon 1:	202 kg/s release for 131s with 1.2 m/s wind speed
Falcon 3:	133 kg/s release for 154s with 3.7 m/s wind speed
Falcon 4:	61 kg/s release for 301s with 4.3 m/s wind speed

Falcon experiments were simulated using the LNG-spill and pool spread/evaporation model. The geometry, including the pond, fences and wall were all implemented into the model. Result can be seen in Figure 22. Gas concentrations are highly under-estimated at the first row of sensors (50m row) in the simulations. Somewhat better results are obtained for the rows at 150m and 250m. The strong under-estimation of gas concentration is due to an inaccurate representation of the source term. Accurately describing the source terms still remains a challenge.

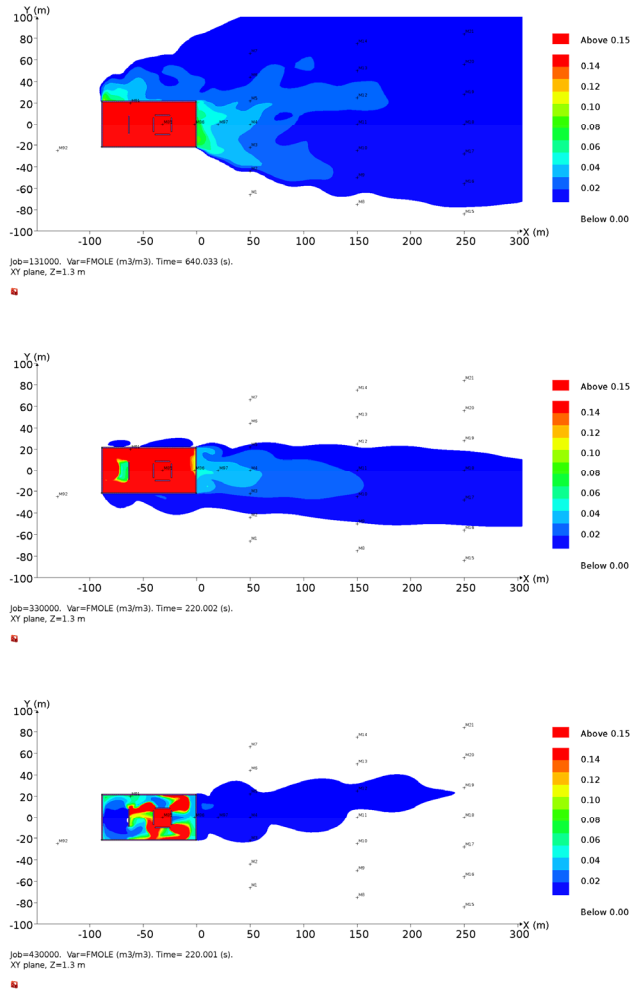

Figure 22: Steady state plume 0.5% contour shown Falcon 1 (top), 3 (middle) and 4 (bottom)

Videos and images indicate that the LNG is released with a certain radial momentum and minimal LNG travels to or evaporates from the middle of the pool. As spilled onto the water the LNG had a relatively high radial velocity (order of 6 m/s) which enhanced the level of turbulence in the fence and the mixing with the water (see Gavelli, 2008). As a result, almost immediately the LNG spill formed a plume of approximately 2-3m in height (estimation from the videos and images). Moreover, on the video of the Falcon 5 test, RPTs can be observed after the fence had been filled up with vapors of LNG. The RPTs projected an important amount of vapor across the fence. Many factors (high radial momentum for the LNG, increased level of turbulence in the fence, possible delayed RPTs) need to be taken into account in order to have an accurate representation of the source term. This work is still in progress. GexCon has tested different modifications of source terms during spills on water, and have developed algorithms that would lead to very good predictions of the Falcon tests with more vertical momentum of vapor near the source. Whether or not these or similar algorithms will be included in future versions of FLACS is currently being evaluated.

CHRC Tests B and C

The details of this test setup as well as simulation setup were presented in the previous section and shown in Figure 11. These simulations were performed at wind-tunnel scale. For both tests 33.9 liter/minute CO_2 (with some propane added) was released through a rectangular source area in a 0.4 m/s wind field.

Measurements were specified at various locations. FLACS simulations agreed quite well with experimental data and the results are shown in Figure 23. Bifurcation, which was observed experimentally for case B, was accurately reproduced by simulations. In addition, a more complex triple peak structure was observed at some arcs for Case C, both experimentally and in the simulations. It should also be noted that when evaluating experimental results, arc concentrations are not always symmetric despite symmetry in the setup.

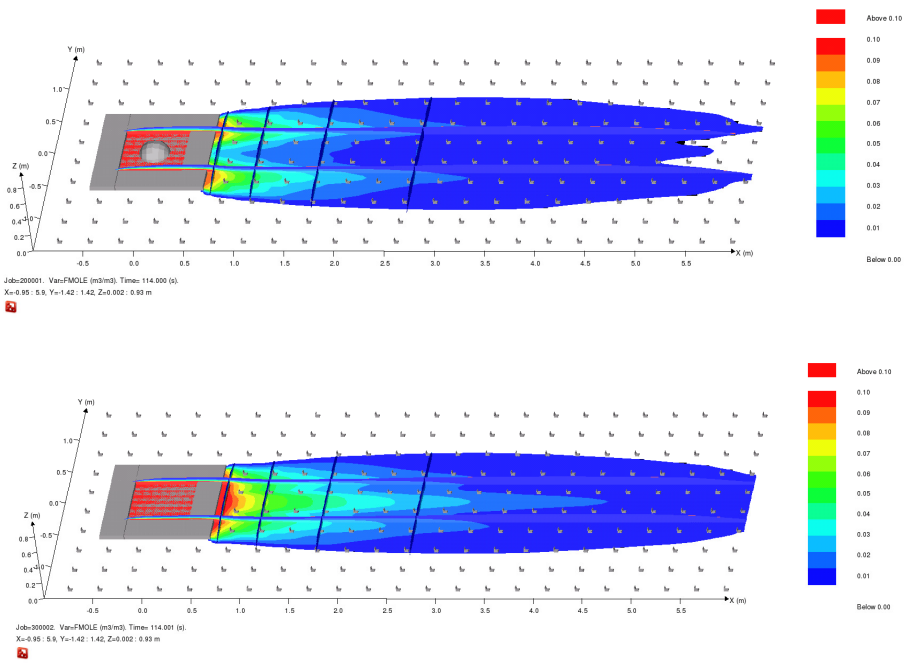

Figure 23: FLACS simulations for CHRC Case B (top) and Case C (bottom)

BA-Hamburg obstructed tests

The BA-Hamburg trials were conducted in an open circuit wind tunnel at the Meteorological Institute at the University of Hamburg and are all continuous releases of sufficient duration that stable statistics were obtained. The tests have been generally described in the previous section for the unobstructed cases. The obstructed cases have incorporated a fence. The fence height was 3 cm. The fence was either semi-circular, or circular, with a diameter of either 19 cm or 30 cm (depending on the test case, and stated in the Model Validation Database), with its centre aligned with the source (see Figure 24). It should be noted that the descriptions in the Model Validation Database and MEP excel-sheet were inaccurate for some of these tests, indicating that diameter of the fence was equal to the distance to the fence. We therefore had to obtain the accurate information in (Nielsen & Ott, 1996). The experiments were at a model scale of 1:164,

equating to a full-scale fence height of approximately 5m. Gas concentration measurements were made at floor level using an aspirated hot film probe.

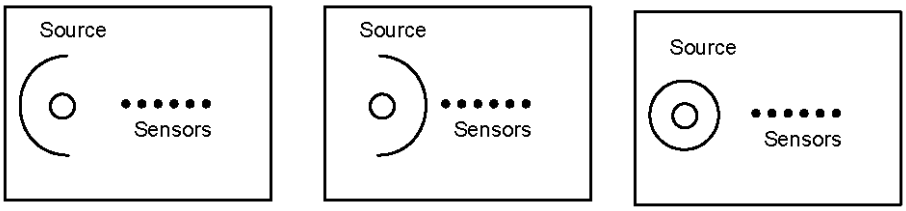

Figure 24: BA-Hamburg obstructed tests: Upwind (left), downwind (middle), and center (right)

FLACS simulations included the geometry as specified in the MEP, but the scaled-up results were used due to the small dimensions in the experiments. Source specified as a diffusive leak from a cylindrical hole (correct diameter 11.48m was used). A 50% porous grid was used in the vertical direction to ensure an upward distributed flow. Flat ground was assumed with a 5m tall fence in the simulations and sensors were defined at ground level (5cm elevation). The wind profile was assumed with 5% turbulence intensity and length scale equal to the smallest grid resolution. The choice of grid for the simulations was: domain (X:-80 to 250-480m, Y: -75 to 75m, Z: -3 to 25m) and the grid resolution for the near field was 1m x 1m x 0.2m. The resulting grid had 240,000 cells, with an approximately 1-day simulation time. For these experiments it was not clearly expressed where experimental measurements were performed (i.e., whether these results were obtained at several locations for each arc distance or only at the centre axis). When evaluating simulation results we concluded that there had to be multiple sensor locations at each arc to explain observations. For the results with the upwind and downwind fences, the maximum arc-concentrations were extracted. For the circular fence experiments, the average values at the downstream locations were extracted due to vortex shedding.

FLACS simulations (Figure 25-Figure 27) were generally in good agreement with experimental data. Some experimental anomalies were observed for the experimental except for test DA0532

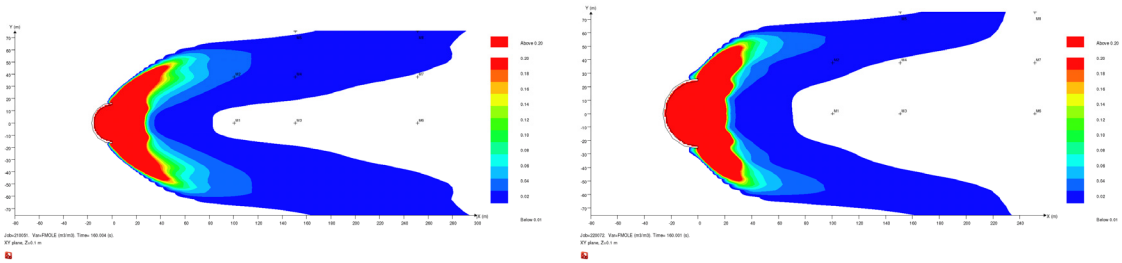

Figure 25: FLACS simulations for tests 039051 and 039072

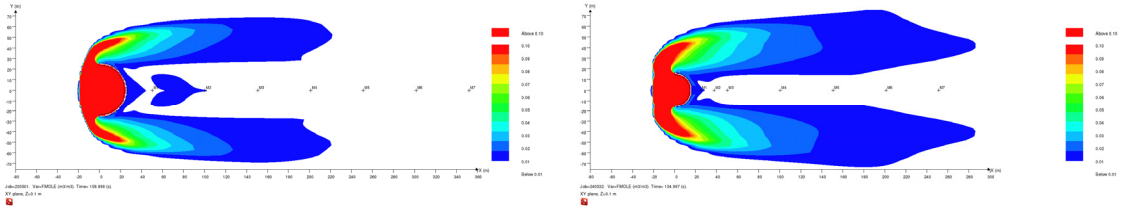

Figure 26: FLACS simulations for tests DA0501 and DA0532

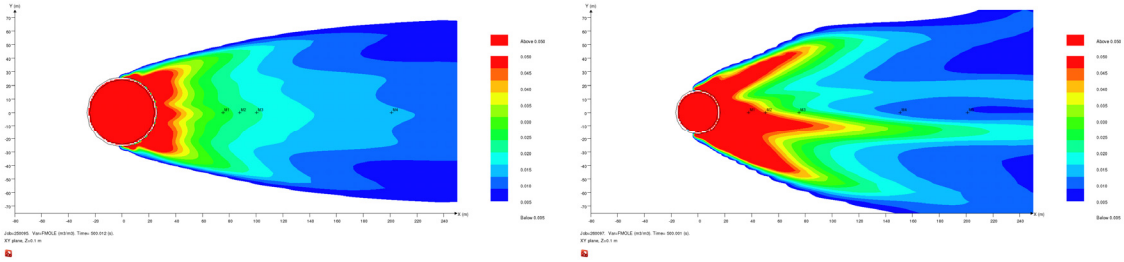

Figure 27: FLACS simulations for tests 039094/039095 and 039097

BA-TNO test TUV02

The general description of the BA-TNO tests was given in the previous section and shown in Figure 17. The TUV01 (unobstructed) and TUV02 wind tunnel experiments at TNO were a 1:78 scale model of a field experiment to investigate the influence of a linear fence perpendicular to the wind direction. Regarding the description in the Model Validation Database, there is no information about the length of the fence. Based on (Nielsen & Ott, 1996) the fence seems to be long, so that all gas will have to pass the fence.

FLACS simulations were implemented for the 78:1 scale-up of the wind-tunnel test, using a diffusive leak (13.4 kg/s) from a cylindrical hole (8.35m diameter). A 50% porous grid in the vertical direction was used to ensure a distributed flow in the upwards direction. Flat terrain was assumed and the wind speed was 5.12 m/s at 0.65m elevation, and the profile used a 10% turbulence intensity and a length scale of 0.2m (2 times the smallest grid size). Sensors were assumed to be at ground level. The choice of grid for the TUV02 simulations was: domain (X:-25 to 100m, Y: -50 to 50m, Z: -3 to 25m) and the grid resolution for the near field was 0.5m x 0.5m x 0.1m (380,000 grid cells or 2-3 CPU days). Experimental results were extracted from monitors defined in the MEP.

While the FLACS simulations yielded decent results when compared to the experimental data, it is still difficult to understand the experimental gas concentration distribution. Similar to the TUV01 experimental results, higher concentrations were reported downwind and downstream the fence in TUV02 (see Figure 28).

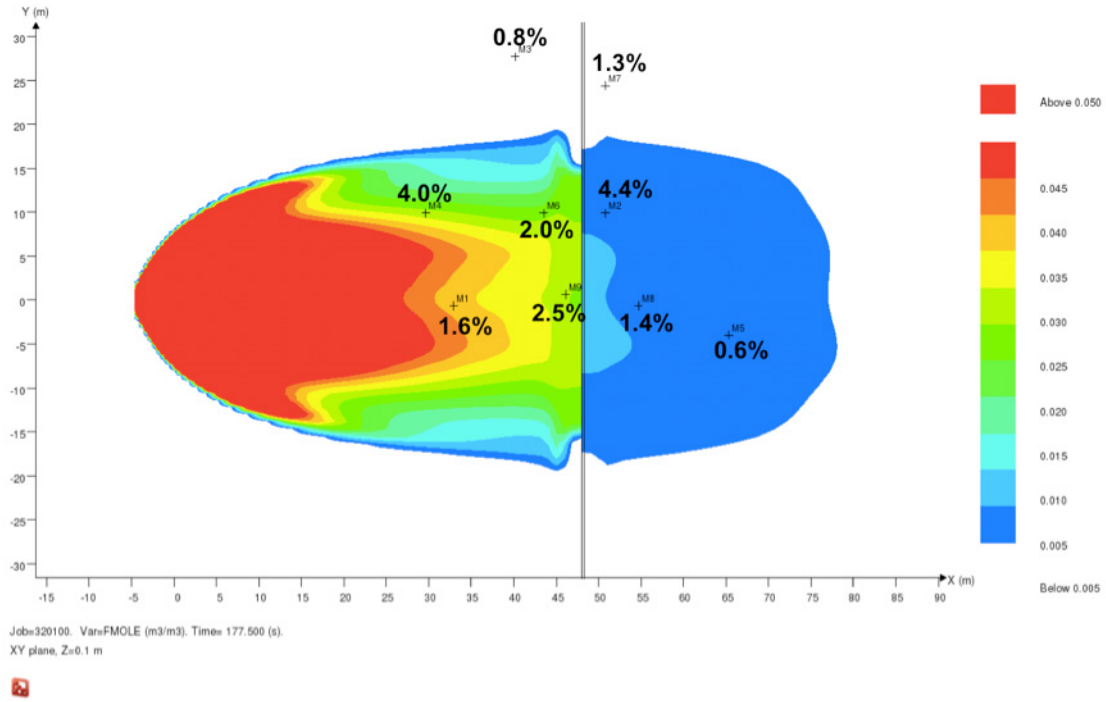

Figure 28: FLACS simulations and experimental data for TUV02 field test

Conclusion

The FLACS CFD tool has been used to simulate all the experimental tests of the Model Validation Database of the MEP. The MEP is used to assess the suitability of dispersion models for predicting hazard ranges associated with large spills of LNG. The models need to be validated against key experimental data which are provided in the Model Validation Database, which consists of both large-scale field trials as well as wind tunnel tests. The 33 tests of the Model Validation Database have been simulated with FLACS. In FLACS a two-dimensional transient spill model is solved simultaneously with a three-dimensional transient flow for the wind. Atmospheric stability is taken into account via the specification of a Pasquill stability class.

Quantitative assessment criteria based on statistical performance measures (SPMs) are given in the MEP. The following quantitative assessment criteria need to be met by a model in order to pass the MEP:

- A mean bias within 50% of the mean corresponding to $-0.4<MRB<0.4$ and $0.67<MG<1.5$
- A scatter of a factor three of the mean corresponding to $MRSE<2.3$ and $VG<3.3$
- The fraction of model observations within a factor of two of observations to be at least 50%

In the above set of criteria MRB denotes Mean Relative Bias, MG denotes Geometric Mean, MRSE denotes Mean Relative Square Error and VG denotes Geometric Variance. The interested reader can find the mathematical expression of these statistical measures in Ivings et al., 2007.

The criteria apply to maximum arc-wise concentrations and plume width data. The set of statistical measures is averaged over all of the test cases.

Below the SPM results obtained with FLACS are shown for Group 1 (unobstructed) and Group 2 (obstructed) benchmark tests. The upper three tables are SPMs for concentration predictions at measurement arcs for: (a) simulations at actual test scale with long averaging times (left), (b) short averaging times (middle), and (c) for wind-tunnel tests modeled at defined full-scale and long averaging times (right). The two lower tables are SPMs for plume width prediction at test scale (left) and for the cases where wind-tunnel tests were modeled at the defined full-scale (right).

SPM for maximum arc-wise concentration for "long" time averages

SPM	Value for unobstructed cases (Group 1)	Value for obstructed cases (Group 2)
MRB	-0,07	0,02
MG	1,10	0,98
MRSE	0,47	0,07
VG	1,82	1,07
FAC2	0,67	1,00

SPM for maximum arc-wise concentration for "short" time averages

SPM	Value for unobstructed cases (Group 1)	Value for obstructed cases (Group 2)
MRB	-0,16	0,00
MG	1,19	0,00
MRSE	0,21	0,00
VG	1,32	0,00
FAC2	0,88	0,00

SPM for maximum arc-wise concentration for "long" time averages

SPM	Value for unobstructed cases (Group 1)	Value for obstructed cases (Group 2)
MRB	-0,13	0,03
MG	1,15	0,97
MRSE	0,24	0,12
VG	1,31	1,13
FAC2	0,85	0,94

SPM for plume width for "long" time averages

SPM	Value for unobstructed cases (Group 1)	Value for obstructed cases (Group 2)
MRB	-0,12	-0,10
MG	1,13	1,11
MRSE	0,19	0,01
VG	1,23	1,01
FAC2	0,93	1,00

SPM for plume width for "long" time averages

SPM	Value for unobstructed cases (Group 1)	Value for obstructed cases (Group 2)
MRB	-0,10	0,00
MG	1,11	0,00
MRSE	0,02	0,00
VG	1,02	0,00
FAC2	1,00	0,00

FLACS successfully met the quantitative criteria as established in the MEP. Possible improvements of the models may lead to even better results in the future. These current efforts include: a better representation of terrain, more accurate representation of experimentally observed meandering winds and more accurate modeling of complex source terms for spills into water, such as those encountered in the Falcon series. This last point will improve ability to predict dispersion from spills into water at low wind speeds.

References

Brown T C, Cederwall R T, Chan S T, Ermak D L, Koopman R P, Lamson K C, McClure J W and Morris, L K, 1990, Falcon series data report: 1987 LNG vapor barrier verification field, Gas Research Institute, Report No. GRI-89/0138, June 1990 (http://www.osti.gov/bridge/servlets/purl/6633087-9HP88a/)

Carissimo B, Jagger S F, Daish N C, et al, 2001, The SMEDIS database and validation exercise, Int J Environment and Pollution, Vol 16, No 1-6, pp 614 – 629.

Coldrick S., Lea C. J. and Ivings M. J., 2009, Validation Database for Evaluating Vapor Dispersion Models for Safety Analysis of LNG Facilities, Guide to the LNG Model Validation Database, The Fire Protection Research Foundation, 24th February 2009

Colenbrander G W, Evans A and Puttock J S, 1984a, Spill tests of LNG and refrigerated liquid propane on the sea, Maplin Sands 1980: Dispersion Data Digest; Trial 27, Shell Research Ltd, Thornton Research Centre, Report TNER.84.028, May 1984.

Colenbrander G W, Evans A and Puttock J S, 1984b, Spill tests of LNG and refrigerated liquid propane on the sea, Maplin Sands 1980: Dispersion Data Digest; Trial 34, Shell Research Ltd, Thornton Research

Centre, Report TNER.84.030, May 1984.

Colenbrander G W, Evans A and Puttock J S, 1984c, Spill tests of LNG and refrigerated liquid propane on the sea, Maplin Sands 1980: Dispersion Data Digest; Trial 35, Shell Research Ltd, Thornton Research Centre, Report TNER.84.031, May 1984.

Conrado, C., Vesovic, V., 2000, The influence of chemical composition on vaporization of LNG and LPG on unconfined water surfaces. Chem. Eng. Sci., 55: 4549-4562

Dharmavaram, S., Hanna, S.R., Hansen, O.R., 2005, Consequence analysis – Using a CFD model for industrial sites. Process Safety Progress 24, 316-327.

Ermak D L, Chapman R, Goldwire H C Jr, Gouveia F J and Rodean H C, 1988, Heavy gas dispersion test summary report, UCRL-21210, Lawrence Livermore National Laboratory, October 1988.

Flaherty J.E. et al, 2007, Evaluation study of building-resolved urban dispersion models, Seventh Symposium on the Urban Environment, 10-13 September 2007.

Gavelli F., Bullister E. and Kytomaa H, 2008, Application of CFD (Fluent) to LNG spills into geometrically complex environments, Journal of Hazardous Materials, (159) 158-168

Goldwire H C Jr, Rodean H C, Cederwall R T, Kansa E J, Koopman R P, McClure J W, McCrae T G, Morris L K, Kamppinen L, Kiefer R D, (Urtiew P A and Lind C D), 1983, Coyote series data report: LLNL/NWC 1981 LNG spill tests dispersion, vapor burn and rapid-phase transitions, Vols 1 & 2, UCID-19953, Lawrence Livermore National Laboratory (https://e-reports-ext.llnl.gov/pdf/195030.pdf and https://e-reports-ext.llnl.gov/pdf/195363.pdf)

Han, J., Arya, S.P., Shen, S. Lin, Y.L., 2000, An estimation of turbulent kinetic energy and energy dissipation rate based on atmospheric boundary similarity theory, Tech. Rep. CR-2000-210298, NASA, USA.

Hanna S R, Strimaitis D G and Chang J C, 1991, Hazard response modelling uncertainty (a quantitative method), Volume II: Evaluation of commonly-used hazardous gas dispersion models, Sigma Research Corporation, Final report, Volume II, April 1989 – April 1991.

Hanna S R, Hansen O R and Dharmavaram S, 2004, FLACS CFD air quality model performance evaluation with Lit Fox, MUST, Praire Grass and EMU observations, Atmospheric Environment, Vol 38, pp 4675 – 4687.

Hanna S.R., Hansen O.R., Ichard M., and Strimaitis D., 2009, Computational Fluid Dynamics (CFD) model simulations of dispersion from chlorine railcar releases in industrial and urban areas, Atmos. Environ., (43) 262-270

Hansen, O.R., Melheim, J.A., Storvik, I.E., 2007. CFD-Modeling of LNG Dispersion Experiments. In: AIChE Spring National Meeting, 7th Topical Conference on Natural Gas Utilization, Houston, USA.

Havens J and Spicer T, 2005, LNG vapor cloud exclusion zones for spills into impoundments, Process Safety Progress, Vol 24, Iss 3, pp 181 – 186.

Havens J and Spicer T, 2006, Vapor dispersion and thermal hazard modelling, Final topical report to Gas Technology Institute under sub-contract K100029184, October 2006.

Havens J, Spicer T and Sheppard W, 2007, Wind tunnel studies of LNG vapor dispersion from impoundments, AIChE National Spring Meeting, Houston.

Hissong D.W., 2007, Keys to modeling LNG spills on water, Journal of Hazardous Materials, (140) 465-477

Ivings M J, Jagger S F, Lea C J and Webber D M, 2007, Evaluating vapor dispersion models for safety analysis of LNG facilities, The Fire Protection Research Foundation, May 9 2007.

Koopman R P, Baker J, Cederwall R T, Goldwire H C Jr, Hogan W J, Kamppinen L M, Kiefer R D, McClure J W, McCrae T G, Morgan D L, Morris L K, Spann M W Jr and Lind C D, 1982b**,** Burro series data report LLNL/NWC 1980 LNG spill tests, UCID-19075, Vols 1 & 2, Lawrence Livermore National Laboratory (https://e-reports-ext.llnl.gov/pdf/194414.pdf and https://e-reportsext.llnl.gov/pdf/194606.pdf)

Koopman R P, Cederwall R T, Ermak D L, Goldwire H C Jr, Hogan W J, McClure J W, McCrae T G, Morgan D L, Rodean H C and Shinn J H, 1982a**,** Analysis of Burro series 40 m^3 LNG spill experiments J Haz Mats, Vol 6, pp 43 – 83.

Koopman R.P., Ermak D.L., 2007, Lessons learned from LNG safety research, Journal of Hazardous Materials, (140) 412-428

Launder, B.E., Spalding, D.B., 1974, The numerical computation of turbulent flows. *Comp. Meth. In App. Mech. And Eng.*, **3**, 269-289.

Luketa-Hanlin, A, 2006, A review of large-scale LNG spills: experiments and modelling, Journal of Hazardous Materials, Vol A132, pp 119 – 140.

Luketa-Hanlin A, Koopman R P and Ermak D L, 2007, On the application of Computational Fluid Dynamics code for liquefied natural gas dispersion, Journal of Hazardous Materials, Vol 140, Iss 3, pp 504 – 517.

McQuaid J (Editor), 1987, Heavy gas dispersion trials at Thorney Island - 2, Proceedings of a symposium held at the University of Sheffield, Great Britain, September 1986, J Haz Mats, Vol 16, pp 1-502.

Nielsen M and Ott S, 1996, A collection of data from dense gas experiments, Riso-R-845 (EN), Riso National Laboratory, Denmark, March 1996.
http://www.risoe.dtu.dk/research/sustainable_energy/energy_systems/projects/rediphem.aspx

Schatzmann M, Marotzke K and Donat J, 1991, Research on continuous and instantaneous heavy gas clouds, Contribution of sub-project EV 4T-0021-D to the final report of the joint CEC-project, University of Hamburg, February 1991.

van den Bosch, C.J.H., Weterings, R.A.P.M., 1997, Methods for the calculation of physical effects due to the release of hazardous materials (liquids and gases), CPR14E, TNO Yellow Book, 3rd edition, TNO, The Hague, The Netherlands.

Webber D M, Gant S E, Ivings M J and Jagger S F, 2009, LNG source term models for hazard analysis, The Fire Protection Research Foundation.